AD
Reports Control Symbol
OSD-1366

RESEARCH AND DEVELOPMENT TECHNICAL REPORT
ECOM-5445

ATMOSPHERIC EFFECTS FOR GROUND TARGET SIGNATURE MODELING

I. Atmospheric Transmission at 1.06 Micrometers

By

Richard B. Gomez

June 1972

ECOM

Reproduced by
NATIONAL TECHNICAL
INFORMATION SERVICE
U S Department of Commerce
Springfield VA 22151

UNITED STATES ARMY ELECTRONICS COMMAND - FORT MONMOUTH, NEW JERSEY

NOTICES

Disclaimers

The findings in this report are not to be construed as an official Department of the Army position, unless so designated by other authorized documents.

The citation of trade names and names of manufacturers in this report is not to be construed as official Government indorsement or approval of commercial products or services referenced herein.

Disposition

Destroy this report when it is no longer needed. Do not return it to the originator.

UNCLASSIFIED
Security Classification

DOCUMENT CONTROL DATA - R & D

(Security classification of title, body of abstract and indexing annotation must be entered when the overall report is classified)

1. ORIGINATING ACTIVITY *(Corporate author)*
Atmospheric Sciences Laboratory
White Sands Missile Range, New Mexico

2a. REPORT SECURITY CLASSIFICATION
Unclassified

2b. GROUP

3. REPORT TITLE
ATMOSPHERIC EFFECTS FOR GROUND TARGET SIGNATURE MODELING
I. Atmospheric Transmission at 1.06 Micrometers

4. DESCRIPTIVE NOTES *(Type of report and inclusive dates)*

5. AUTHOR(S) *(First name, middle initial, last name)*
Richard B. Gomez

6. REPORT DATE	7a. TOTAL NO. OF PAGES	7b. NO. OF REFS
June 1972	47	78

8a. CONTRACT OR GRANT NO.	9a. ORIGINATOR'S REPORT NUMBER(S)
b. PROJECT NO.	ECOM-5445
c. DA Task No. 1T061102B53A-19	9b. OTHER REPORT NO(S) *(Any other numbers that may be assigned this report)*
d.	

10. DISTRIBUTION STATEMENT
Approved for public release; distribution unlimited.

11. SUPPLEMENTARY NOTES	12. SPONSORING MILITARY ACTIVITY
	U. S. Army Electronics Command Fort Monmouth, New Jersey

13. ABSTRACT

The results of a literature search and subsequent theoretical analysis conducted to determine the characteristics of atmospheric transmission at 1.06 micrometers wavelength are presented. The effects of molecular scattering, molecular absorption, aerosol scattering, and aerosol absorption are considered. Atmospheric transmission at 1.54 micrometers is compared with the transmission at 1.06 micrometers. In addition, problem areas which must be resolved to enable one to make adequate transmission predictions are brought out in this report. It is concluded that aerosol scattering is the primary attenuating mechanism on 1.06 micrometers radiation; for all practical purposes, losses due to molecular absorption, molecular scattering, and aerosol absorption seem small and negligible compared to the loss due to aerosol scattering. For horizontal paths at sea level with good visibility (>10 km) the total extinction coefficient lies in the range of 2×10^{-2} to 2×10^{-1} km^{-1}. Attenuation due to rain over short paths (<5 km) and for rain rates less than 10 mm/hr is not severe; however, cloud, fog, and haze will have a considerable effect on the transmission. Atmospheric transmission at 1.06 μm and 1.54 μm is higher than at most of the other laser wavelengths available; however, spectral measurements are not currently available with high enough resolution to decide which of these two wavelengths has a higher transmission.

DD FORM 1 NOV 68 1473 REPLACES DD FORM 1473, 1 JAN 64, WHICH IS OBSOLETE FOR ARMY USE.

UNCLASSIFIED
Security Classification

14. KEY WORDS	LINK A		LINK B		LINK C	
	ROLE	WT	ROLE	WT	ROLE	WT
1. Optics 2. Electromagnetics 3. Lasers 4. Transmittance 5. Attenuation						

Reports Control Symbol
OSD-1366

Technical Report ECOM-5445

ATMOSPHERIC EFFECTS FOR GROUND TARGET SIGNATURE MODELING

I. Atmospheric Transmission at 1.06 Micrometers

By

Richard B. Gomez

Atmospheric Sciences Laboratory
White Sands Missile Range, New Mexico

June 1972

DA Task No. 1T061102B53A-19

U. S. Army Electronics Command

Fort Monmouth, New Jersey

CONTENTS

FIGURES

TABLES

1. INTRODUCTION

This is the first of a series of reports to be prepared in support of the atmospheric modeling portion of a comprehensive Ground Target Signature (GTS) modeling program. The aim of the atmospheric modeling project is to develop the capability of predicting atmospheric effects on ground target signatures for a wide range of meteorological conditions. Accomplishment of this objective will provide the information required for the design and operation of terminal homing, target acquisition, and surveillance systems. It will also influence the choice of operating wavelengths for artificial sources used in conjunction with these systems [1]. Moreover, it will provide the knowledge needed to discriminate between target and environmental effects [1].

The neodymium (Nd^{3+}) laser wavelength of 1.06 μm was chosen for this initial investigation because the Nd^{3+} laser is currently being employed in laser guided terminal homing missile systems [2]. The purpose of this report is to present the results of a literature search (through January 1972) and theoretical analysis conducted to determine the characteristics of atmospheric transmission at the 1.06 μm wavelength. The last literature survey on the subject was conducted by Roy and Emmons [3] in 1965, but analysis of atmosphere effects on the propagation of 1.06 μm Nd^{3+} laser radiation has been treated more recently [4-6].

Results of experimental and theoretical transmission studies by various investigators are used to estimate the transmission characteristics for 1.06 μm radiation. The atmospheric effects of molecular and aerosol scattering and absorption are treated. Other effects, such as turbulence, multiple scattering, nonlinearity, and quantum mechanical corrections are neglected, although under certain experimental conditions these effects may be significant (e.g., transmission through a heavy cloud layer where multiple scattering becomes significant or high beam intensity where nonlinear effects are important). Transmittance models which include some of these effects at various wavelengths including 1.06 μm will be treated in subsequent reports in this series.

Section 2 is a discussion of Nd^{3+} laser emission and a quantitative description of atmospheric effects on laser radiation. Problem areas which need to be resolved to enable one to make reliable transmission predictions are brought out in this section.

Section 3 is a discussion and analysis of the results of both experimental and theoretical transmission studies made by various investigators in the region of interest.

Section 4 is a comparison between atmospheric transmission at 1.06 μm and 1.54 μm, since transmission at these two wavelengths is higher than at most other laser wavelengths available [6].

Section 5 is a summary of the report, includes some concluding remarks, and provides the results of Section 3 in tabular form.

2. BACKGROUND

2.1 Neodymium Laser Emission Spectral Characteristics

Neodymium (Nd) lasers are receiving much attention for use in atmospheric laser systems because of their emission spectral characteristics that lie in a region for which the atmosphere is relatively transparent, and because they can be operated at ambient temperature with high efficiency. The trivalent neodymium ion (Nd^{3+}) is the active entity of these lasers that operate at or near 1.06 μm wavelength, with some finite linewidth. In describing their spectral characteristics, it is necessary to differentiate between the gross and fine structure of the emission bands [7]. The gross structure of the emission bands (the generation wavelength) is dependent on the host material and on the concentration of the doping material [8]. The fine structure of the emission bands is mainly dependent on the resonator properties and on the width and character of the luminescence line broadening [7]. The important types of neodymium lasers commonly being used in atmospheric laser systems are Nd:YAG and Nd:glass. These two lasers are briefly discussed below.

An Nd:YAG laser requires relatively low threshold pumping power and can be operated in either a continuous wave (CW) or pulsed mode with reasonably high powers. Ytterium aluminum garnet (YAG) as a host material is hard, has a high thermal conductivity, and can be grown with good optical quality [8]. The laser generation wavelength is at 1.065 μm with linewidths of about 10Å [8]. Models emitting up to one kilowatt continuous power at 1.06 μm are commerically available [9].

Characteristics of Nd:glass lasers are discussed in great detail in the literature [10-14]. The major disadvantage of glass as a host material is its low thermal conductivity [10]. This imposes limitations on the diameter that can be used for CW and high repetition rate operations because the glass host cannot dissipate heat quickly. An important factor which strongly influences the generation spectrum is the character of the luminescence line broadening in the active medium [7]. For an inhomogeneously broadened luminescence, the width of the laser emission spectrum can be quite large. Due to the nature of the glass host, line broadening in neodymium glass is inhomogeneous [7,10]. Snitzer [15] reports that the Nd^{3+} 1.06 μm glass laser emission envelope just above threshold is approximately 3×10^{-4} μm wide but can be increased to approximately 1.3×10^{-2} μm by increasing the pump power. He further reports that individual laser modes of widths less than 10^{-5} μm can be obtained anywhere within this 1.3×10^{-2} μm wide emission evelope. Hence, the

spectral composition of the Nd:glass laser varies within a single flash [16]. Since the Nd:glass laser has a high energy storage per unit volume and the glass host material affords considerable flexibility in size and shape, very high output powers are realizable from the Nd:glass laser [10,11].

2.2 Transmittance

In this report the simplified model [17] of an atmosphere composed of N plane parallel homogeneous layers, each characterized by an extinction coefficient, γ_j, will be adopted but not applied to the 1.06 μm wavelength because of lack of experimental data concerning aerosol and molecular extinction coefficients versus altitude at this wavelength. The application of this model which considerably reduces the complexity of the problem of calculating the atmospheric transmittance of radiation will be the subject of subsequent reports in this series. The complexity of the problem is due to the dependence of the extinction coefficient on a number of different physical properties of the atmosphere [18]. In essence, this plane stratified atmospheric model requires that the physical properties of the atmosphere change with elevation, but not laterally and in addition requires that the curvature of the earth be neglected.

Consider a beam of monochromatic collimated laser radiation propagating along the path $\Delta\ell_j$ in the jth layer of the assumed plane stratified atmosphere. The transmittance τ_j is given by

$$\tau_j = \exp(-\gamma_j \Delta\ell_j) \tag{1}$$

where

$$\Delta\ell_j = \Delta Z_j \sec\theta. \tag{2}$$

Here ΔZ_j represents the increment of vertical distance and θ is the angle between the vertical and the direction of propagation. The total transmittance of this model atmosphere is given by

$$\tau = \prod_{j=1}^{N} \tau_j \tag{3}$$

or

$$\tau = \exp\left(-\sum_{j=1}^{N} \gamma_j \Delta\ell_j\right). \tag{4}$$

The extinction coefficient γ_j can be expressed as the sum of the scattering coefficient σ_j and the absorption coefficient k_j, i.e.,

$$\gamma_j = \sigma_j + k_j. \tag{5}$$

The quantities σ_j and k_j depend on the kind and number of molecules and aerosols in the atmospheric path (see section 2.6), so one can write

$$\sigma_j = \sigma_{mj} + \sigma_{aj} \tag{6}$$

and

$$k_j = k_{mj} + k_{aj} \tag{7}$$

where

σ_m = molecular scattering coefficient

σ_a = aerosol scattering coefficient

k_m = molecular absorption coefficient

k_a = aerosol absorption coefficient.

All of the above coefficients, γ, σ, and k, are defined in km^{-1} if $\Delta\ell$ is in kilometers (km).

2.3 Molecular Scattering

The molecular scattering (Rayleigh) coefficient, σ_m, as a function of altitude for each wavelength, is expressed by

$$\sigma_m(h,\lambda) = \sigma_R(\lambda)N(h) \tag{8}$$

where

$\sigma_R(\lambda)$ = Rayleigh cross section at wavelength λ

$N(h)$ = molecular number density at altitude h.

Equation (8) is used to compute the Rayleigh coefficient, σ_{m_j}, characterizing the jth layer located at an altitude h. The Rayleigh cross sections for anisotropic air molecules is computed from [19]

$$\sigma_R(\lambda) = \frac{8\pi^3 (n^2-1)^2}{3\lambda^4 N^2} \cdot f \tag{9}$$

where $f = 3(2+\delta)/(6-7\delta)$, δ is the so-called depolarization factor, n is the index of refraction of air, and N is the molecular number density at sea level.

The factor f is included in Equation (9) to compensate for the degree of molecular anisotropy. Gucker and Basu [20] report a value of .035 for δ.

The index of refraction for "standard air," viz., dry air containing 0.03 percent by volume of CO_2 at a pressure of 1013.25 mb and a temperature of 288°K, may be computed from the dispersion formula of Edlen [21],

$$(n-1)10^6 = 64.328 + \frac{29498.10}{146-(\lambda^{-2})} + \frac{255.40}{41-(\lambda^{-2})} \qquad (10)$$

where λ is the wavelength in micrometers. In terms of atmospheric pressure P(mb) and temperature T(°K) the refractive modulus $(n-1)10^6$ may be given by a less precise but more convenient formula [22], i.e.,

$$(n-1)10^6 = \frac{77.6P}{T} + \frac{0.584P}{T\,\lambda^2} . \qquad (11)$$

Equation (11) is valid for wavelengths from 0.2 μm to 20 μm.

2.4 Selective Molecular Absorption

The absorption bands of the atmospheric gases constitute a complex superposition of many spectral lines; therefore, one writes

$$k_{mj}(\nu) = \sum_i k_{mij}(\nu) \qquad (12)$$

where k_{mij} is the molecular absorption coefficient of the ith spectral line in the jth layer. The (i) summation is over all molecular absorption lines of all absorbing species which are close enough to the wavenumber ν to contribute significantly to the total molecular absorption coefficient $k_{mj}(\nu)$.

The attenuation of laser radiation in the atmosphere is caused in part by the so-called continuum absorption due primarily to the integrated effects of the wings of nearby strong absorption lines. This decomposition of the molecular absorption coefficient, $k_{mj}(\nu)$, may be expressed in the form

$$k_{mj}(\nu) = \sum_r k_{mrj}(\nu) + \sum_s k_{msj}(\nu) \qquad (13)$$

where the "r" summation is over all spectral lines whose centers are within the spectral width $\Delta\nu$ of the laser radiation and the "s" summation extends to all absorbing species beyond the limits of $\Delta\nu$ which affect

the transmission in $\Delta\nu$. The first term is the total selective molecular absorption coefficient. The second term is the continuum molecular absorption contribution from the wings of the many distant absorption lines on either side of the spectral region under consideration. The definition of the term "total continuum absorption coefficient" is discussed in the following section.

The molecular absorption coefficient $k_{mij}(\nu)$ for a collision-broadened line can be given to good accuracy in the lower layers of the atmosphere (altitude <50 km) for the pressure range from about 10^3mb to about 10 mb by [23]

$$k_{mij}(\nu) = \frac{S_{ij}\,\alpha_{ij}}{\pi}\left[\frac{1}{(\nu-\nu_{oij})^2 + \alpha_{ij}^2}\right] \tag{14}$$

where

$$S_{ij} = \int k_{mij}(\nu)\,d\nu. \tag{15}$$

Here S_{ij} is the normalized line intensity, α_{ij} is the half-width at half maximum, ν_{oij} is the wavenumber determining the position of the center of the ith spectral line and ν is the wavenumber at which the absorption coefficient is required. The Lorentz line shape given by Equation (14) is valid for ν lying within a few tenths of a cm^{-1} of the line center ν_{oij} [24]. It has been shown [24] that when $(\nu-\nu_{oi})>>\alpha_i$ the wings of the lines decay much more rapidly than Lorentz lines. Hence, for continuum molecular absorption calculations, a correction factor must be introduced into the Lorentz shape when ν lies beyond a few tenths of a cm^{-1} from the line center ν_{oi}. Line shape studies are needed in order to find the correct form for $k_m(\nu)$ that would be valid for all ν.

The line intensities are functions of temperature, the dependence being different for different spectral lines. If S_o is the value of intensity at standard temperature, T_o, and pressure, P_o, the value of S at other temperatures is given by [25]

$$S(T,p) = S_o p (T_o/T)^a \exp\left\{(-E''/k)\left[\frac{T_o - T}{T_o T}\right]\right\} \tag{16}$$

where

E'' = energy of molecule in the lower state of the transition responsible for the spectral line
k = Boltzmann's constant
p = partial pressure of absorbing gas (in atmospheres)
T = temperature (in degrees Kelvin)
a = constant depending on absorbing gas.

The half-width of the absorption line is a function of the partial pressure of the absorbing gas, the pressure of the nonabsorbing gas, and the temperature. The temperature and pressure dependence of the half-width is approximately [25]

$$\alpha = \alpha_o \left(\frac{P_e}{P_o}\right)\left(\frac{T_o}{T}\right)^b . \qquad (17)$$

Here α_o is the half-width of the line in question at a pressure P_o and a temperature T_o. The constant b depends on the absorbing gas. The effective pressure P_e is usually determined from the empirical relation [26]

$$P_e = P + (B-1)p \qquad (18)$$

where P is the total atmospheric pressure; p is the partial pressure of the absorbing gas; and B is the self-broadening factor defined as the ratio of the self-broadening to the broadening by the nonabsorbing gas present. For small amounts of absorbers under atmospheric conditions $P >> p$ so that one can write $P_e \approx P$.

Calculations of the integrated transmittance over the rotational bands of water vapor have shown that the temperature dependence of this quantity is determined mainly by the temperature dependence of the line intensities [27]. The temperature variation of the line intensity may change by several orders of magnitude for the temperature range that occurs in the atmosphere [28]. At 1.06 μm the vibration-rotation bands dominate absorption so a corresponding study of the effects of temperature and pressure on the half-widths and intensities of vibrational-rotational lines is needed in order to predict accurately what these effects will do to radiation propagating through a real atmosphere under any weather conditions.

At present it is difficult to determine experimentally the fine structure of the vibrational-rotational spectrum (such as line positions, their intensities, and half-widths) for the majority of lines [29]. The experimental difficulties are caused by the abundance of absorption lines, their overlapping, and the spectrometer's slit function which makes it impossible to determine the true line contours and masks weak narrow lines. However, line strengths and half-widths may, in principle, be calculated from quantum mechanics, although in practice the calculations are intractable. An attempt to predict the fine structure of vibrational rotational spectra theoretically has been made by Gates et al. [30] for the 2.7 μm band of H_2O. Although the authors took the positions of the line centers from experimental data, the intensities and half-widths were calculated by quantum mechanical methods. However, they did not consider the interaction of vibrational and rotational motions of the molecule. Failure to take into account the vibrational-rotation interaction in

water vapor may result in errors amounting from ten to several hundred per cent [31]. Zuev et al. [29,32] have taken into account the vibration-rotation interaction in calculating the intensities, half-widths, and line centers by quantum mechanical methods. The very high degree of monochromaticity of laser radiation makes this degree of sophistication necessary in calculating absorption of laser radiation in the atmosphere. This is true for the neodymium laser whose emission evelope can be relatively broad (as wide as 1.3×10^{-2} μm) because the individual laser modes within the envelope may have widths less than 10^{-5} μm [15]. Presently, to this author's knowledge, no quantum mechanical calculations for the molecular absorption coefficient at $\lambda = 1.06$ μm for any absorbing gas have been reported in the literature.

2.5 Total Continuum Absorption

Practically all attempts at experimental investigation of the total continuum absorption have been made in the 8-12 μm window. Even here, the results of the total continuum effect are rather contradictory. The absorption coefficients calculated by various authors for the 8-12 μm spectral region differ by 50 to 100% [33]. One of the major problems is that the definition of the total continuum absorption coefficient is vague. That is due to the fact that attenuation in the so called "atmospheric windows" caused by the continuum molecular absorption due to wind effects of nearby strong absorbing lines is just one of the components of the overall continuum attenuation of the radiation. There is also attenuation of radiation due to molecular scattering, aerosol absorption, aerosol scattering, and in the case of highly monochromatic lasers, there may be strong selective molecular absorption by atmospheric gases such as H_2O, O_2, CO_2, and O_3. Hence, in many cases all of these attenuation factors are lumped into one and the total continuum absorption coefficient k_T^c in the spectral width $\Delta\nu$ is defined by the equation [33]

$$\exp\{-k_T^c \ell\} = \frac{1}{\Delta\nu}\int_{\Delta\nu} \exp\{-\Sigma_j \gamma_j \Delta\ell_j\} d\nu \tag{19}$$

where

$$\ell = \Sigma_j \Delta\ell_j$$

is the total path and the extinction coefficient, γ_j, includes all the following terms:

$$\gamma_j = \sigma_{mj} + \Sigma_r k_{mrj} + \Sigma_s k_{msj} + \sigma_{aj} + k_{aj}. \tag{20}$$

Many authors simply assume that all but the third term of Equation (20) are negligible or that the attenuation effect in the atmospheric window $\Delta\nu$ is caused solely by the molecular absorption by wings of nearby lines.

The continuum absorption coefficient k_j^c is defined in this report as equivalent to the continuum molecular coefficient given by (See Equation (13))

$$k_j^c = \sum_s k_{msj} \quad .$$

The total continuum absorption coefficient in the spectral interval for this case is calculated from

$$\exp\{-k_T^c \ell\} = \frac{1}{\Delta\nu} \int_{\Delta\nu} \exp\{-\sum_j k_j^c \Delta\ell_j\} d\nu. \tag{21}$$

The quantity k_j^c is evaluated at a position, far removed from the centers of the absorbing lines, where the line variations with wavenumbers are small in the interval $\Delta\nu$. Hence, the summation

$$\sum_j k_j^c \Delta\ell_j$$

may be treated to a first approximation as constant in the spectral interval $\Delta\nu$ so that

$$k_T^c = \frac{1}{\ell} \sum_j k_j^c \Delta\ell_j. \tag{22}$$

In order to measure k_T^c as defined by Equation (22), the effects due to the other attenuation components (see Equation (20)) must be considered.

The problem of the temperature dependence of absorption in the continuum is not established [33]. The dependence of k^c(on temperature and pressure should be resolved if predictions of continuum effects are to be made for different weather conditions.

2.6 Aerosol Extinction: Attenuation of Radiation at 1.06 μm Wavelength by Dust, Haze, Fog, Cloud, Rain, and Snow

The transmission of near-infrared radiation through the atmosphere is largely dependent on scattering and absorption by the most variable and least investigated atmospheric component, the atmospheric aerosol. The aerosol may consist of dust and combustion products, salt particles, industrial pollutants, minute living organisms and, most important, water droplets.

Mie theory can be used to derive the aerosol absorption (k_a) and scattering (σ_a) coefficients for spherical particles (or some other simple forms), provided the complex index of refraction, number density and size distribution are specified. One should keep in mind, however, that irregu-

larities in particle shape will disrupt the resonance inside the particle causing marked changes in the scattering [34]. Very few studies have been made under controlled conditions to compare the calculated and experimentally measured coefficients of radiation attenuation by the aerosol [35,36].

An assumption which is often made is that absorption by the scattering aerosol particles is negligibly small. Since over most of the spectrum aerosol scattering encountered in the atmosphere is dominant over aerosol absorption, this assumption is reasonable. However, there are exceptions where the scattering particles absorb strongly [37] so that one has to be careful in practice before making this assumption. In what follows, the aerosol absorption coefficient will be assumed negligible and thus the terms "aerosol extinction coefficient" and "aerosol scattering coefficient" may be used interchangeably. Areas where the magnitude of aerosol absorption may be significant will be indicated.

The atmospheric aerosol is present in any stratum in the atmosphere but with a highly variable concentration both in space and time. The aerosol size distribution spans a large range of particle sizes and may have considerable structure as found by Fenn [38], Goetz [39], Kondrat'yev et al. [40], and Rozenburg [41]. Moreover, many of the natural aerosol particles which are mixtures of water-soluble and water-insoluble components will undergo severe size fluctuations as the relative humidity varies [42,43]. The natural aerosol particles vary in size from about 4×10^{-3} μm radius to about 10^{2} μm radius and are generally classified as follows:

a. Aitken particles of radius $\sim 10^{-3}$ to 10^{-1} μm

b. Large particles of radius $\sim 10^{-1}$ to 1.0 μm

c. Giant particles of radius $\gtrsim$ 1.0 μm.

The Aitken particles have the distinction of having a strongly wavelength-dependent absorption spectrum [41].

If the atmospheric aerosol is treated as spherical particles, the attenuation of radiation by aerosol will depend on the particle composition, the particle size distribution, and the number density. Consider an atmosphere where the aerosol sizes within a unit volume are characterized by a size distribution function f(r). Various size distribution functions have been offered in the literature to describe the real atmosphere (e.g., Junge [44], Fenn [38], Fortzik [45]). The aerosol attenuation coefficient γ_a is given by

$$\gamma_a(h, n, r, \lambda) = \int_{N_{r_1}}^{N_{r_2}} C_s(n, r, \lambda) dN(r) \qquad (23)$$

where

$$dN(r) = N(h)f(r)dr; \quad \int_{r_1}^{r_2} f(r)dr = 1 \tag{24}$$

and $dN(r)$ = number of particles with radii between r and r+dr per unit volume

γ_a = aerosol extinction coefficient

n = complex index of refraction

λ = wavelength of incident radiation

C_s = cross section for each particle

r_1, r_2 = minimum and maximum radii of the aerosol particles

$N(h)$ = total number of particles with radii between r_1 and r_2 per unit volume at height h

$f(r)$ = size distribution function

N_{r_1} & N_{r_2} = aerosol number density limits corresponding to the limits r_1 and r_2.

So

$$\gamma_a(h,n,r,\lambda) = N(h) \int_{r_1}^{r_2} C_s(n,r,\lambda)f(r)dr. \tag{25}$$

This is usually written in terms of the efficiency factor Q_{ext} defined as the ratio of the aerosol cross section C_s to the geometrical cross section of a single particle πr^2:

$$Q_{ext} = C_s(n,r,\lambda)/\pi r^2. \tag{26}$$

Hence, Equation (24) can be given as

$$\gamma_a = N \int_{r_1}^{r_2} \pi r^2 Q_{ext}(n,r,\lambda)f(r)dr., \tag{27}$$

From Equation (5) it is seen that γ_a is given by

$$\gamma_a = \sigma_a + k_a \tag{28}$$

where each of the coefficients γ_a, σ_a, and k_a can be written in terms of the sum of the corresponding ith particle coefficients:

$$\gamma_a = \sum_{i=1}^{N} \gamma_{ai}$$

$$\sigma_a = \sum_{i=1}^{N} \sigma_{ai} \qquad (29)$$

$$k_a = \sum_{i=1}^{N} k_{ai} \, .$$

These definitions of γ_a, σ_a, and k_a are rigorous only if multiple scattering is ignored [46]. General expressions for Q_{ext} follow from Mie theory.

The widely varying aerosol characteristics which represent a specific atmospheric condition and are needed for the theoretical calculations of the extinction coefficient are difficult to measure in practice. Hence, the most effective method for obtaining the spectral variation of the aerosol extinction coefficients is by direct measurement of aerosol attenuation of radiation at various wavelengths and for different atmospheric conditions. [47,48].

3. PUBLISHED DATA

In this section the published results of transmission measurements and theoretical calculations are used to estimate the atmospheric effects on the propagation of 1.06 μm laser radiation. The only available transmission data at this wavelength was obtained with apparatus having limited spectral resolution and therefore the results of this section are first-order approximations. The atmospheric attenuating mechanisms for which data are presented are molecular scattering, molecular line absorption, molecular continuum absorption, and attenuation by the aerosol. Quantitative estimates of the effects of haze, fog, cloud, and rain are provided. Finally, a qualitative estimate of attenuation by snowfall is included.

3.1 Molecular Scattering (σ_m)

Elterman [19] has tabulated the theoretical values of molecular scattering coefficients for a clear standard atmospheric model for altitudes up to 50 km. Twenty-two wavelengths between 0.27 and 4.0 μm are considered. The meteorological range at sea level corresponds to about 25 km at 0.55 μm wavelength. The meteorological range or visual range, V, is that distance for which the transmittance falls to 2%, i.e., $V = 3.1912/\beta$ where β is the total scattering extinction coefficient. Figures 1 and 2 are plots of σ_m versus λ and γ_a versus λ based upon Elterman's data [19]. From these data it is seen that the molecular scattering coefficient for 1.06 μm wavelength radiation should be of the order of 8.2×10^{-4} km^{-1} at sea level and approximately 6.1×10^{-4} km^{-1} at an altitude of 3 km.

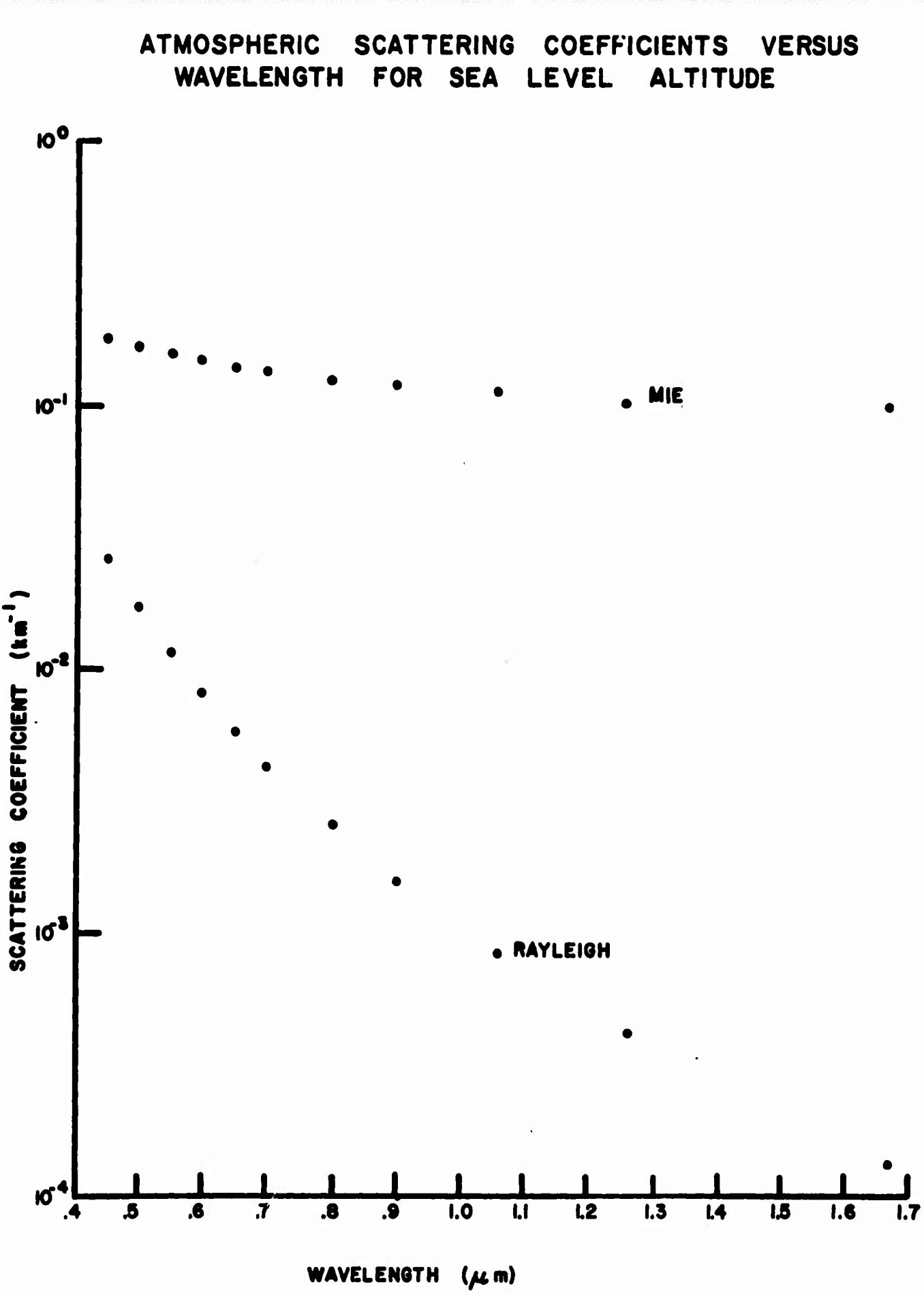

Figure 1. Rayleigh and aerosol scattering coefficients at sea level as a function of wavelength (from data by Elterman [19]).

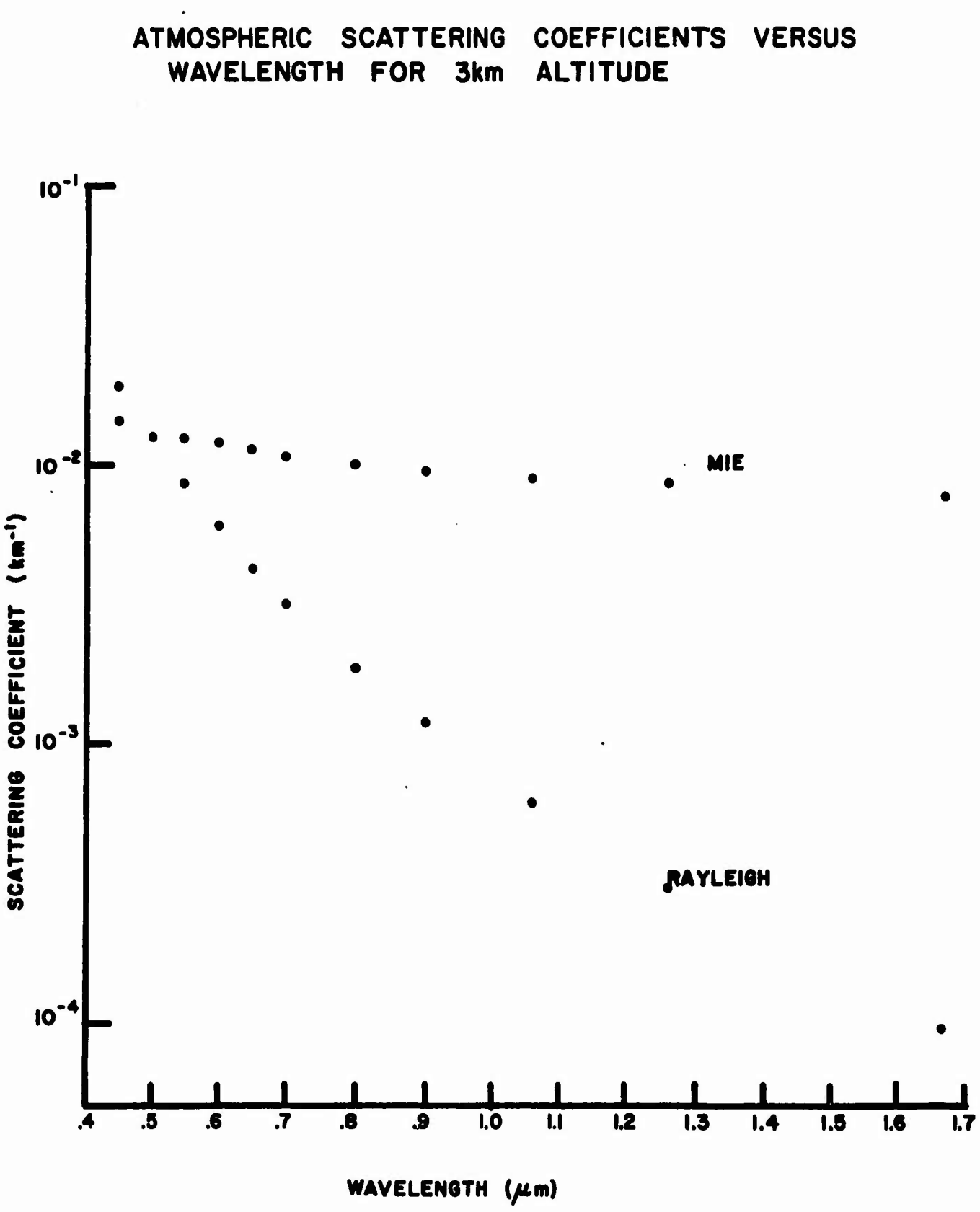

Figure 2. Rayleigh and aerosol scattering coefficients at 3 km altitude as a function of wavelength (from data by Elterman [19]).

These are of the same order as the values obtained for the molecular scattering coefficient σ_m by McClatchey et al. [17] for 1.06 μm radiation along a path for five different atmospheric models (see Table 1). It will be seen that the contribution to the overall attenuation of 1.06 μm radiation from the Rayleigh component is small and may be ignored for path lengths less than 10^2 km.

3.2 Selective Molecular Absorption (k_m)

The atmosphere is exceptionally free of strong absorption lines in the 1.06 μm region as is evident from solar spectra [49,50]. Only a few weak O_2 and H_2O lines and the short-lived $[O_2]_2$ and $[O_2\text{-}N_2]$ complexes are active in this region. These lines are difficult to observe in the laboratory even with high resolution and long paths (~2 km).

Figures 3-9 are facsimiles of plates 26 to 29 from the Mohler Solar Atlas [49]. A scale can be arbitrarily set to indicate relative absorption. No observations were made through cloudy or hazy skies. An upper bound on the absorption coefficient may be obtained for the maximum selective line absorption coefficient by use of these data. The strongest absorption line shown is located at 10585.1Å. If one assumes an equivalent 16 km sea-level path and a minimum transmittance of 35% on the arbitrary scale based on Taylor and Yates data [51], Equation (1) yields for this line (assuming all attenuation is due to line absorption):

$$k_m^{max} \sim 6.5 \times 10^{-2} \text{ km}^{-1}.$$

From a superficial examination of the spectrum, it appears that the average baseline transmittance over a 10Å bandwidth is of the order of 95%. This yields a molecular absorption coefficient for this region of the order of

$$k_m^{base} \sim 3 \times 10^{-3} \text{ km}^{-1}.$$

It seems reasonable to expect the line absorption contribution to the total extinction coefficient to fall between these two limits. A statistical analysis by Zuev et al. [52] of atmospheric transparency to laser radiation at various wavelengths reveals that the absorption coefficient k_m is small, not exceeding

$$k_m \sim 4 \times 10^{-2} \text{ km}^{-1}$$

at 1.06 μm under the conditons of Temperature = 283°K and precipitable-centimeters (pr-cm) of H_2O = 0.3 to 0.7.

TABLE I

Molecular scattering coefficients reported by McClatchey et al. [17] for 1.06 μm wavelength for five different atmospheric models.

Altitude (km)	Tropical $\sigma_m(km^{-1})$	Midlatitude Summer $\sigma_m(km^{-1})$	Midlatitude Winter $\sigma_m(km^{-1})$	Subarctic Summer $\sigma_m(km^{-1})$	Subarctic Winter $\sigma_m(km^{-1})$
0	8.04E-04	8.20E-04	8.91E-04	8.38E-04	9.39E-04
0-1	7.68E-04	7.81E-04	8.43E-04	7.98E-04	8.77E-04
1-2	6.99E-04	7.06E-04	7.52E-04	7.21E-04	7.70E-04
2-3	6.33E-04	6.38E-04	6.70E-04	6.50E-04	6.82E-04

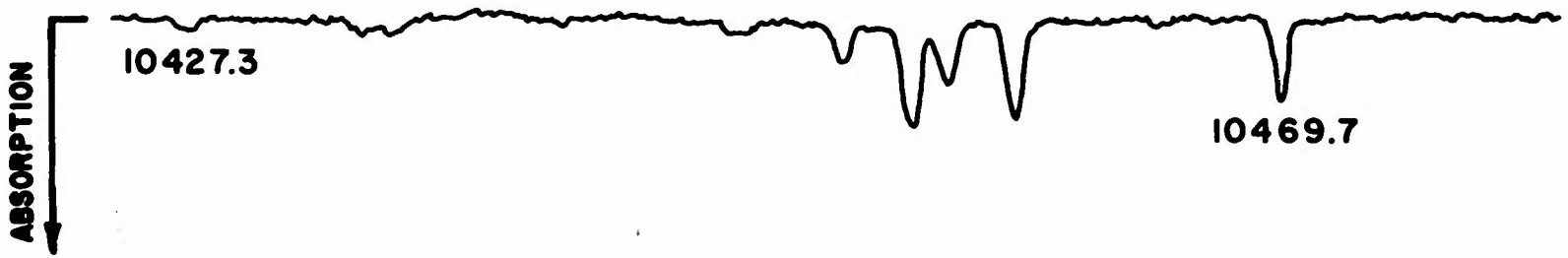

Figure 3. Atmospheric absorption lines between 10,427.3Å and 10,469.7Å (from reference [49]).

Figure 4. Atmospheric absorption lines between 10,469.7Å and 10,513.0Å (from reference [49]).

Figure 5. Atmospheric absorption lines between 10,513.0Å and 10,532.2Å (from reference [49]).

Figure 6. Atmospheric absorption lines between 10,532.2Å and 10,585.1Å (from reference [49]).

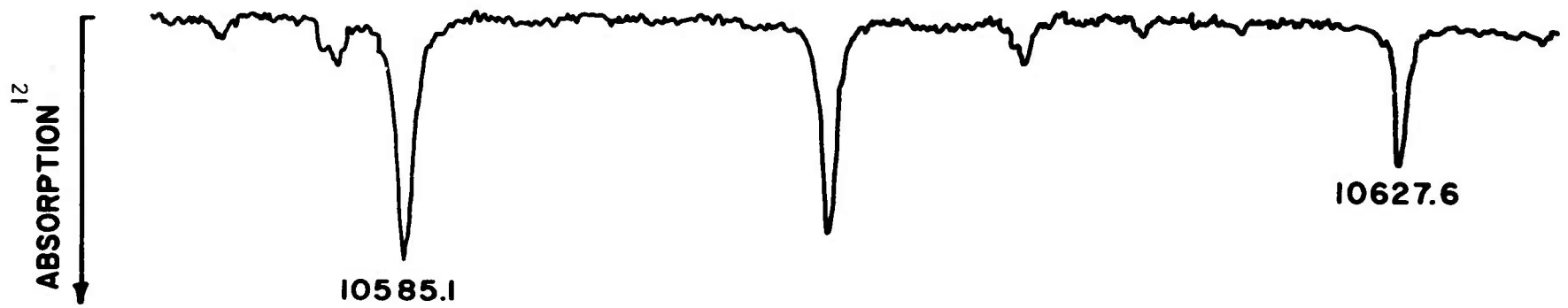

Figure 7. Atmospheric absorption lines between 10,585.1Å and 10,627.6Å (from reference [49]).

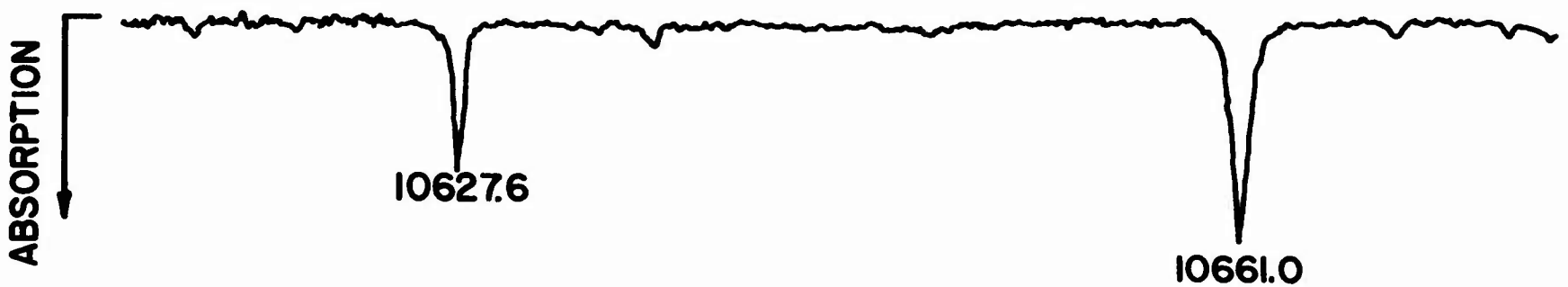

Figure 8. Atmospheric absorption lines between 10,627.6Å and 10,661.0Å (from reference [49]).

Figure 9. Atmospheric absorption lines between 10,661.0Å and 10,707.4Å (from reference [49]).

The contribution by the $[O_2]_2$ and $[O_2\text{-}N_2]$ complexes has been under investigation by Dianov-Klokov et al.[53]. They have shown that the role of the band of the $[O_2]_2$ complex at 1.064 μm is dominant over the role of the individual O_2 molecules. Additional data on the bands of the complexes in the near-infrared are needed to account for radiation loss due to these bands.

3.3 Total Continuum Absorption (K_T^c)

There is practically no experimental data concerning the water vapor continuum in the region for $\lambda<8\mu m$ except at the two points λ = 3.70 μm and λ = 3.58 μm where $k_T^c = 0.062$ gm^{-1} cm^2 and $k_T^c = 0.07$ gm^{-1} cm^2, respectively [54]. A quantitative assessment by Andreyev and Gal'tsev [33] of the continuum absorption coefficient for the region $\lambda<8\mu m$, based on the numerical analysis of the fine structure data of the water vapor spectrum presently available results in

$$k^c_{1.06} \sim 2 \times 10^{-3} \text{ gm}^{-1} \text{ cm}^2$$

or

$$k^c_{1.06} \sim 6 \times 10^{-26} \text{ molecules}^{-1} \text{ cm}^2$$

or

$$k^c_{1.06} \sim 1.6 \times 10^{-6} \text{ (atm-cm)}^{-1}_{\text{STP}}.$$

To evaluate the contribution of k_T^c to the total extinction coefficient computed from Taylor and Yates' data [51] in a later section of this report, consider the path length to be 16 km, the temperature to be 278°K and the relative humidity (RH) to be 40%, so that one has

$$k_T^c \sim 6 \times 10^{-4} \text{ km}^{-1}.$$

This is of the order of the Rayleigh coefficient σ_m, although at 305°K and 70% relative humidity, k_T^c will be an order of magnitude greater.

The coefficient of continuum absorption by H_2O for $\lambda \sim 1.06$ μm computed by Kozyrev and Bazhenov [55] from experimental data of Elder and Strong [56] and Streete [57] on the attenuation of radiation in the water vapor windows results in

$$k^c_{1.06} \sim 5 \times 10^{-2} \text{ gm}^{-1} \text{ cm}^2$$

or

$$k^c_{1.06} \sim 1.5 \times 10^{-24} \text{ molecules}^{-1} \text{ cm}^2$$

or

$$k^{c}_{1.06} \sim 4 \times 10^{-5} \text{ (atm-cm)}^{-1}_{STP}.$$

At 278°K and 48% relative humidity one has

$$k^{c}_{1.06} \sim 1.5 \times 10^{-2} \text{ km}^{-1}.$$

This value extrapolated from available experimental data is 25 times greater than the theoretical value.

In the above cases it is not clear how the total continuum absorption coefficient k^{c}_{T} is defined. This may be the reason for such a large discrepancy between these two values. The largest value $k^{c}_{T} = 1.5 \times 10^{-2}\text{km}^{-1}$ seems somewhat of an overestimate but is useful as an upper limit for k^{c}_{T} at T = 278°K and RH = 48%. At T = 291°K and RH = 55%, this limit increases to $k^{c}_{T} = 4 \times 10^{-2}\text{km}^{-1}$. Thus it is seen that k^{c}_{T} is a function of temperature and relative humidity.

3.4 Aerosol Extinction: Attenuation of Radiation at 1.06 μm Wavelength by Dust, Haze, Fog, Cloud, Rain, and Snow

McCormick, Lawrence, and Crownfield [58] calculated backscattering and total cross sections for a Junge [44] size distribution f(r) of spherical aerosol particles with a refractive index of 1.5. These calculations were made for incident laser radiation at wavelengths of 0.3472 μm, 0.5300 μm, 0.6943 μm, and 1.06 μm, for different values of the size distribution parameter where

$$f(r) = br^{-(v+1)}; \; b = \text{constant}$$

and for four sets of particle radii limits (r_1, r_2). Only the aerosol component was considered in their computations. For v = 3 and (r_1 = 0.04 μm, r_2 = 10.0 μm), their results for the average scattering cross sections per particle, $\bar{C}_s$, at the different wavelengths are

$$\bar{C}_s \; (\lambda = 0.3472 \text{ μm}) = 2 \times 10^{-10}\text{cm}^2$$
$$\bar{C}_s \; (\lambda = 0.5300 \text{ μm}) = 1.32 \times 10^{-10}\text{cm}^2$$
$$\bar{C}_s \; (\lambda = 0.6943 \text{ μm}) = 1.01 \times 10^{-10}\text{cm}^2$$
$$\bar{C}_s \; (\lambda = 1.06 \text{ μm}) = 6.56 \times 10^{-11}\text{cm}^2 \; . \; .$$

If a "clear" atmosphere (23 km visibility), is assumed, the particle density at sea level is given by McClatchey et al. [17] approximately as 2.8×10^3 particles cm^{-3} so that the average scattering coefficients computed from McCormick et al. [58] data are

$$\bar{\sigma}_a \ (\lambda = 0.3472\ \mu m) \sim 5.6 \times 10^{-2} km^{-1}$$
$$\bar{\sigma}_a \ (\lambda = 0.5300\ \mu m) \sim 3.7 \times 10^{-2} km^{-1}$$
$$\bar{\sigma}_a \ (\lambda = 0.6943\ \mu m) \sim 2.8 \times 10^{-2} km^{-1}$$
$$\bar{\sigma}_a \ (\lambda = 1.06\ \mu m) \sim 1.8 \times 10^{-2} km^{-1} .$$

It is seen that the average scattering coefficient for $\lambda = 1.06$ μm is smaller than the scattering coefficients at the shorter wavelengths. It may be additionally inferred that if aerosol scattering is the dominant mechanism for reducing the transmission, the 1.54 μm wavelength should have a higher transmission.

Curcio, Knestrick, Cosden, and Drummeter [59] have reported on the attenuation of radiation by aerosol scattering. They reached the conclusion that the effective particle-size distribution for a particular day at any location near the coast can generally be approximated by a combination of continental and maritime distributions [60]. A typical measured relationship between the atmospheric aerosol extinction coefficient γ_a and the wavelength for a particular day in the Chesapeake Bay area is shown in their paper [59]. They corrected the data to show only the attenuation due to the atmospheric aerosol. From their data, the aerosol extinction coefficient at $\lambda = 1.06$ μm for a 16 km path and 25 km visibility is approximately given by

$$\gamma_a \sim 1.13 \times 10^{-1} \ km^{-1} \qquad \begin{matrix} T = 291°K;\ RH = 55\% \\ pr\text{-}cm \text{ of } H_2O = 4. \end{matrix}$$

From Elterman's data [19], it is seen (Figures 1 and 2) that in the 1.06 μm wavelength region, the Rayleigh scattering coefficient σ_m is of no importance as compared with the aerosol extinction coefficient γ_a. The value for $\gamma_a(\lambda = 1.06\ \mu m)$ as given by Elterman (for meteorological range = 25 km) is $\gamma_a \sim 1.13 \times 10^{-1} km^{-1}$.

Following is a discussion of results concerning the attenuation of 1.06 μm wavelength radiation by important types of aerosols: humid haze, fog, cloud, rain, and snow. Experimental measurements of attenuation by dry dust and other aerosols not included in the above types are not presented because of lack of data. Realistic theoretical estimates of dry particles such as these (dust, industrial pollutants, etc.) cannot be made because these particles are very irregular in shape. Irregular particles, as mentioned in Section 2.6, do not scatter radiation in entirely the same way that spherical particles do and hence Mie theory is not applicable. The water envelope on aerosols tends to make the spherical shape assumption more realistic, although how realistic is open to question.

Haze is defined as that finely dispersed fraction of the atmospheric aerosol with particle radius sizes lying between 0.1 μm to 0.6 μm. Hazes are formed when the relative humidity is less than 80%. When the relative humidity increases to about 80% or greater, a haze is replaced by a foggy haze, which in turn is replaced by a fog as the saturation point is reached. The essential characteristic of a fog as well as for a foggy haze is the existence, against the background of a continuous particle size distribution, of two stable narrow ranges of average sized particles [48]. For foggy hazes the ranges of particle radii are 1 to 5 μm and 12 to 15 μm, while for fogs, they are 8 to 12 μm and 18 to 25 μm. The radii of the droplets that dominate the scattering characteristics by clouds are between 5 and 20 μm. The average radii for rain droplets exceed 100 μm.

Approximately 90 to 95% of the aerosol formations characterizing the state of the atmosphere under real meteorological conditions are hazes [48]. Rosenburg [48] reports that a Junge size distribution should not be used to calculate extinction coefficients in the case of humid hazes, because of the water envelope. According to Gebbie et al. [61] and Sinclair [62], natural haze is approximately transparent in visible and near-infrared regions, and according to Arnulf et al. [63] the transmission increases markedly with increasing wavelength, from the visible to 10 μm. Arnulf et al. measured the transmittance τ through haze by use of the expression

$$\tau = 10^{-dx}$$

where d is the optical density per unit length and x is the atmospheric path length. The optical densities and extinction coefficients obtained by Arnulf et al. for the case of haze are shown in Figure 10. The optical densities, d, are related to the extinction coefficients by

$$\gamma = 2.3d.$$

At 1.06 μm the densities fall in the interval $1\ km^{-1} > d > 0.5\ km^{-1}$. The extinction coefficient, γ_{haze}, in this case lies in the interval

$$2.3\ km^{-1} > \gamma_{haze} > 1.15\ km^{-1}$$

indicating that for a 1 kilometer path, the transmittance τ falls in the interval

$$10\% < \tau < 32\%.$$

The value for γ computed by Arnulf et al. probably also includes absorption by the haze, because it has been shown by Robinson [64] and Kondratyev [65] that it is likely that haze not only scatters, but also absorbs significantly in the visible and infrared spectral regions.

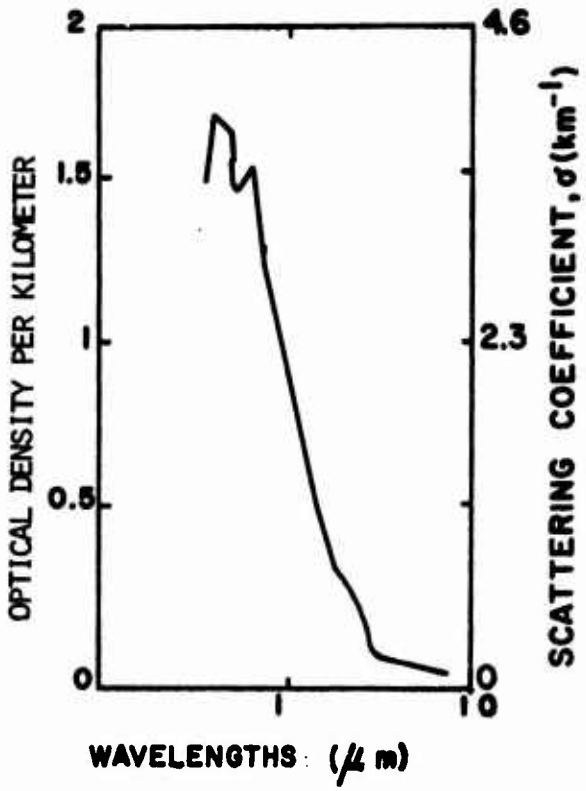

Figure 10. Scattering coefficients and optical densities for the case of haze (from reference [63]).

Arnulf et al. [63] also investigated the extinction of radiation by fogs. Figure 11 gives the extinction coefficients and optical densities of several types of fogs as compiled by them. As seen from the figure, a particular stable fog exhibits approximately the same opacity at all wavelengths shown out to 4 μm at which point it becomes more transparent. Moreover, the transmittance of the various fogs at 10 μm is observed to be higher than at all other wavelengths shown in the figure. It should be noted that the mean radii of the droplets of most fog investigated by Arnulf et al. fall in the range 2.3 to 3.0 μm, which is substantially less than the results of other investigators. The maximum measured drop radius never exceeded 15 μm.

Kurnick, Zitter, and Williams [66] measured the transmittance of natural fogs at various wavelengths and found a monotonic decrease of the extinction coefficient with wavelength.

The controversy as to what degree the optical properties of fogs determined experimentally with special chambers containing artificial fogs can be used to predict transmission through natural fogs has not yet been resolved [67,68].

Gates and Shaw [69] measured transmission through various cloud types using the sun as a source. They report that transmission through clouds is always slightly higher in the 8.0 to 12.0 μm wavelength region than in the 0.48 to 5 μm wavelength region. Since calculations of pure scattering by clouds show better transmission at the shorter wavelengths than at the longer wavelengths, the authors conclude that the water vapor bands in the near infrared absorbed sufficiently to reverse the trend.

Carrier, Cato, and Von Essen [70] computed extinction coefficients for eight specific cloud models using the exact Mie theory for incident radiation at wavelengths of 0.488, 0.694, 1.06, 4.0 and 10.6 μm. Their results showed that there is no clear advantage of one wavelength over another for improving through-cloud transmission, although backscattering is markedly reduced at the longer wavelengths. The largest source of uncertainty of their results is the neglect of multiple scattering. Table II is a summary of calculated extinction coefficients versus wavelength for the eight models considered. Wide variations in these values can be expected for cloud models that differ from those used in this investigation.

Scattering by rain is a multiple scattering phenomenon which is difficult to analyze quantitatively. However, an estimate of attenuation by rain can be made by assuming single scattering theory and by taking notice that multiple scattering effects will only lower the measured extinction coefficient. Thus, by Equation (27), i.e.,

$$\gamma_{rain} = N \int_{r_1}^{r_2} \pi r^2 Q_{ext}(n,r,\lambda) f(r) dr \qquad (30)$$

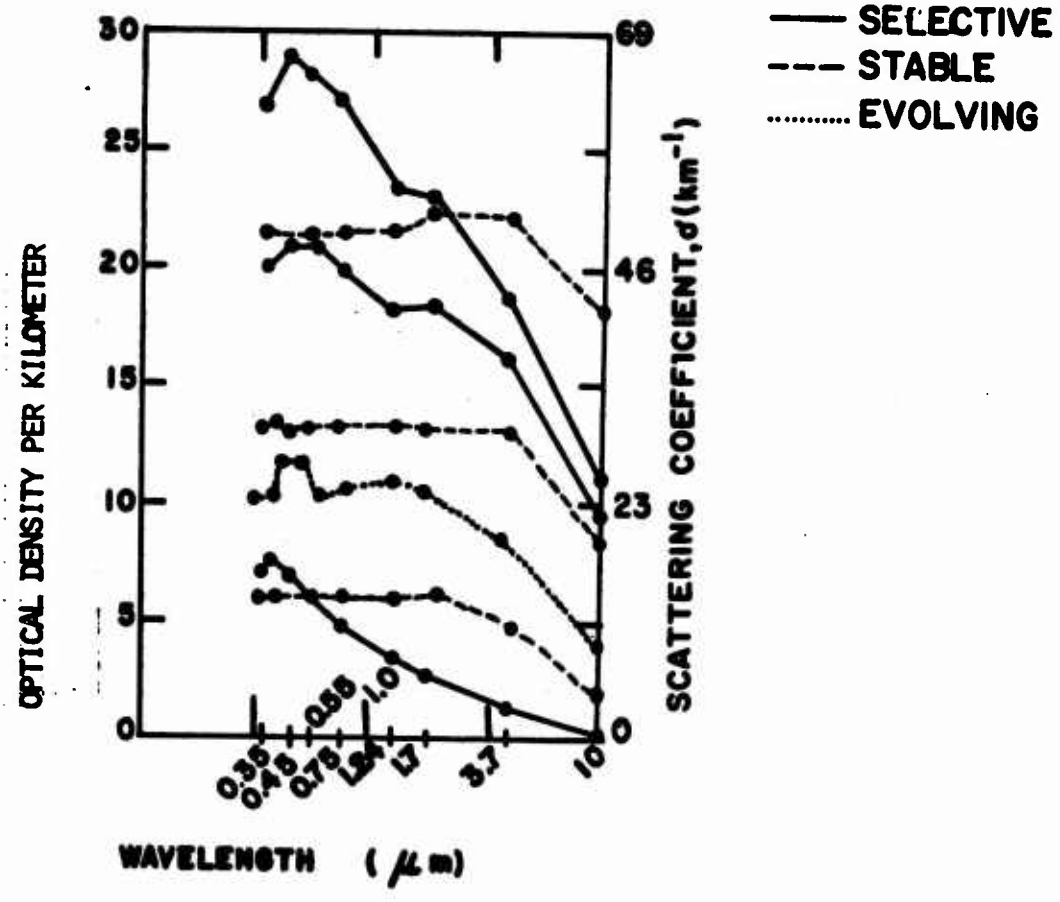

Figure 11. Scattering coefficients and optical densities for the case of fog (from reference [63]).

TABLE II

Extinction coefficients versus wavelength for eight specific cloud types (from reference [70]).

	EXTINCTION COEFFICIENT γ (km^{-1}) Wavelength				
Cloud Type	0.488 μm	0.694 μm	1.06 μm	4.0 μm	10.6 μm
Nimbostratus	128	130	132	147	136
Altostratus	108	109	112	130	83.9
Stratus II	100	101	103	114	104
Cumulus Congestus	69.2	69.8	71.3	81.0	67.6
Stratus I	66.9	67.9	69.7	90.1	42.8
Cumulonimbus	43.5	43.8	44.4	48.2	50.9
Stratocumulus	45.3	46.0	47.1	59.6	24.8
Fair Wx Cumulus	21.0	21.3	21.9	27.6	11.7

an approximate upper bound for the extinction coefficient for rain can be found for a given concentration N. Now at wavelengths between 0.4 μm and 15 μm, the rain drops can be considered as large droplets with Q_{ext} virtually equal to two.

Hence,

$$\gamma_{rain} = 2N \int_{r_1}^{r_2} \pi r^2 f(r)dr = 2G. \tag{31}$$

Here

$$G = N \int_{r_1}^{r_2} \pi r^2 f(r)dr \tag{32}$$

is the geometrical cross section of drops in unit volume. Thus the extinction coefficient for rain given by Equation (31) is independent of wavelength between 0.4 μm and 15 μm.

Polyakova [71] has shown from experimental studies that the magnitude of γ_{rain} from 0.4 to 15 μm wavelength can be obtained from rainfall intensity data. Polyakova established the empirical relationship

$$\gamma_{rain} = 0.21J^{0.74} \tag{33}$$

where J is the rainfall rate in mm/hr and γ_{rain} is the magnitude of the extinction coefficient for rain in units of km^{-1}. Figure 12 gives rainfall rate versus attenuation by rain for near infrared wavelengths.

The extinction coefficient for rain can thus be estimated from Equation (31) if the analytical form of the drop size distribution and the drop number density are known or, from Equation (33), if the rainfall intensity is known.

The value for γ_{rain} (λ = 1.06 μm) calculated by Equation (33) for 1 mm/hr rate of rainfall is

$$\gamma_{rain}(\lambda = 1.06\ \mu m) = 2.1 \times 10^{-1}\ km^{-1}$$

and for 10 mm/hr rate of rainfall

$$\gamma_{rain}\ (\lambda = 1.06\ \mu m) = 1.15\ km^{-1}.$$

Snow consists of scatterers of very complex form; this makes theoretical predictions of attenuation at different wavelengths extremely difficult. Although the extinction coefficient for rain is independent of wavelength

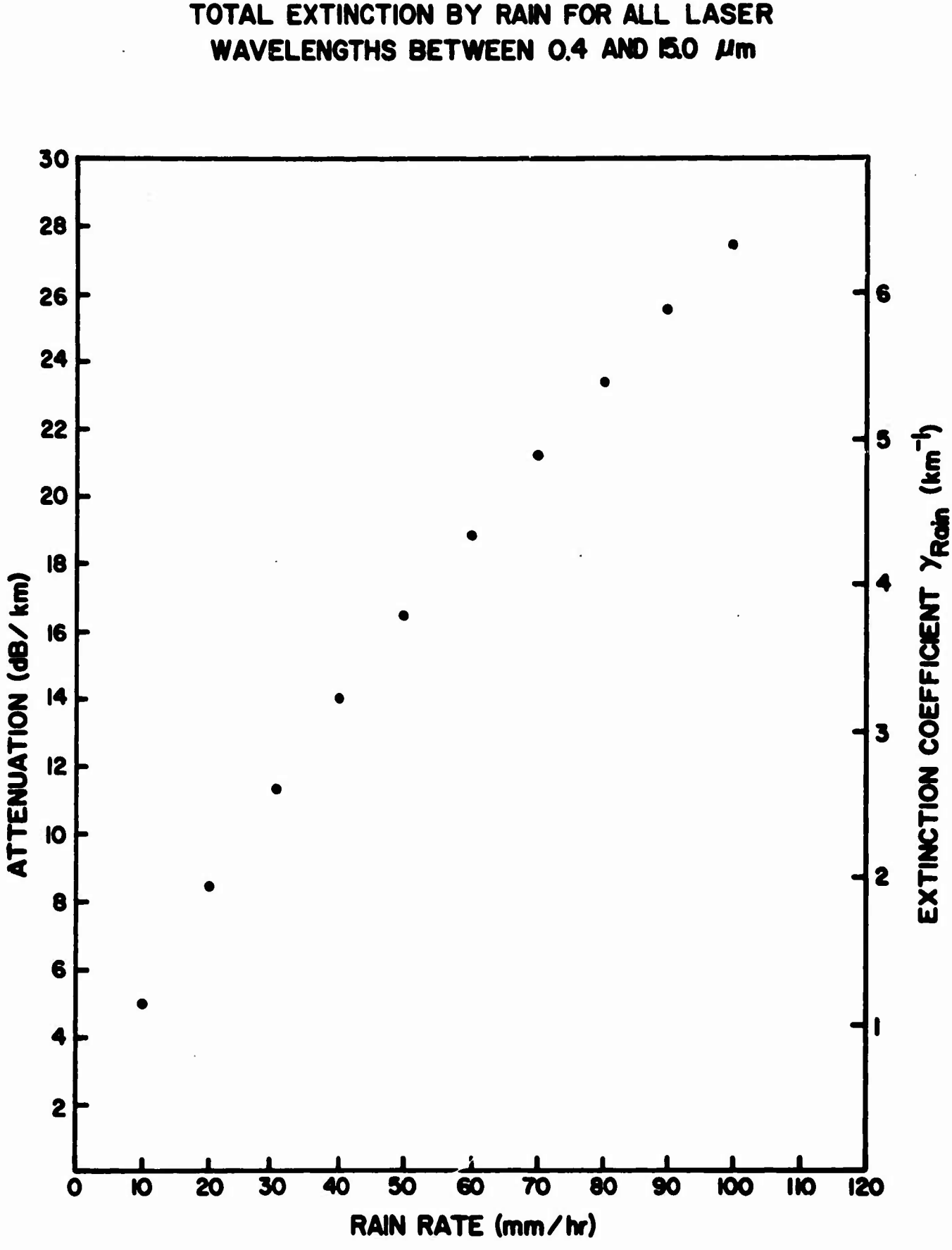

Figure 12. Rainfall rate (mm/hr) versus attenuation (dB/km).

between 0.4 μm and 15 μm, the same is not true of snow. Wilson and Penzias [72] have observed the wavelength dependence of the measured attenuation coefficient in snowfall where they found that the attenuation is greater at 10 μm wavelength than at 0.63 μm or 3.5 μm wavelength. Measurements by Kabanov and Pkhalagov [73] indicate that attenuation by snowfall at 10 μm wavelength is greater than at 1 μm wavelength. (Attenuation is still severe at 1 μm wavelength, about between that due to fog and that due to rain for the same amount of equivalent liquid water [74].) This suggests that transmission through snowfall is better at 1.06 μm (Nd^{3+} laser) than at 10.6 μm (CO_2 laser) wavelength. This inference has not yet been experimentally tested.

There are few experimental data available on the aerosol attenuation coefficient $\gamma_a(h)$ in the infrared at various altitudes at the present time [75].

4. COMPARISON BETWEEN TRANSMISSION AT 1.06 μm AND 1.54 μm

Berlinguette and Tate [76] have made spectroscopic measurements of absolute transmission for atmospheric paths for the wavelength region 0.9 μm to 5.9 μm with horizontal path lengths of 0.67 km and 1.2 km. Selective window transmissions, in terms of precipitable water vapor, were established for the 0.92 μm to 1.10 μm window and other spectral windows for path lengths of 0.007 km, 0.01 km, 0.27 km, 0.67 km, and 1.2 km. The amounts of precipitable water in the paths considered varied from 0.02 to 7.4 mm. Unfortunately, errors of ±3% appeared to be involved in the calibration of their apparatus so that little reliance can be placed on the absolute scale of their transmission plots. One can, however, compare the value of the extinction coefficients for 1.06 μm neodymium (Nd^{3+}) and 1.54 μm erbium (Er^{3+}) laser radiation from their data. For the longest path (1.2 km) with resolving power of about 200 at 1.06 μm wavelength and 7.4 precipitable millimeters of water vapor in the path, their data show that

$$\gamma_{1.06} \sim 1.13 \times 10^{-1} \text{ km}^{-1}$$

$$\gamma_{1.54} \sim 4.3 \times 10^{-2} \text{ km}^{-1} .$$

That is,

$$\gamma_{1.06} \sim 2.6\gamma_{1.54}.$$

In terms of precipitable mm of H_2O:

$$\gamma_{1.06} \sim 1.8 \times 10^{-2} \text{ mm}^{-1}(H_2O)$$

compared to the erbium case (atmospheric transmission characteristics of Er^{3+} discussed in reference [77])

$$\gamma_{1.54} \sim 6.9 \times 10^{-3} \text{ mm}^{-1}(H_2O).$$

Taylor and Yates [51] have made infrared transmission measurements from 0.5 μm to 15 μm wavelength over three horizontal sea-level paths of 0.305 km, 5.5 km, and 16.25 km at Chesapeake Bay. Figure 13 displays their results for a relatively clear winter day under the conditions shown. They covered the band 0.5 μm to 1.8 μm with a resolving power of 353 at 1.06 μm. The extinction coefficients calculated from their data for both Nd^{3+} and Er^{3+} laser wavelengths are

a) 5.5 km path: $\gamma_{1.06} \sim 1.15 \times 10^{-1} \text{ km}^{-1}$

$\gamma_{1.54} \sim 7.8 \times 10^{-2} \text{ km}^{-1}$

or in terms of precipitable water vapor in the path:

$\gamma_{1.06} \sim 4.63 \times 10^{-2} \text{ mm}^{-1}$ (H_2O)

$\gamma_{1.54} \sim 3.14 \times 10^{-2} \text{ mm}^{-1}$ (H_2O)

b) 16.25 km path: $\gamma_{1.06} \sim 6.3 \times 10^{-2} \text{ km}^{-1}$

$\gamma_{1.54} \sim 4.7 \times 10^{-2} \text{ km}^{-1}$

or in terms of precipitable water vapor in the path:

$\gamma_{1.06} \sim 2.0 \times 10^{-2} \text{ mm}^{-1}$ (H_2O)

$\gamma_{1.54} \sim 1.5 \times 10^{-2} \text{ mm}^{-1}$ (H_2O).

R. K. Long [6] has examined transmission measurements made by Streete [57]. At medium resolution, the data indicated that transmission at 1.06 μm may be higher than that at 1.54 μm. This is at odds with the results of this report which are based essentially on Taylor and Yates data. However, at higher resolution, Streete's data indicated that the absolute transmittances are comparable and transmission at 1.536 and 1.544 μm may be higher. The conclusion of the author corroborates that of Long [6] that Streete's data are not any more accurate than those of Taylor and Yates. Thus the problem regarding the transmission at 1.06 μm vs 1.54 μm is still unresolved. In any case, it is safe to say, transmission at these two wavelengths is higher than at most of the other laser wavelengths available. The problem of which wavelength has a higher transmission awaits higher resolution experimental studies at these two wavelengths.

CURVE	PATH LENGTH	DATE	TIME	TEMP.	R.H.	PRECIPITABLE WATER	VISUAL RANGE
A	1000'	3-20-56	3PM	37°F	62%	1.1MM	22MI.
B	3.4MI.	3-20-56	10PM	34.5°F	47%	13.7MM	16MI.
C	10.1MI.	3-21-56	12AM	40.5°F	48%	52.0MM	24MI.

WINDOW DEFINITIONS

I	0.72 TO 0.94μ	V	1.90 TO 2.70μ
II	0.94 TO 1.13μ	VI	2.70 TO 4.30μ
III	1.13 TO 1.38μ	VII	4.30 TO 6.0 μ
IV	1.38 TO 1.90μ	VIII	6.0 TO 15.0 μ

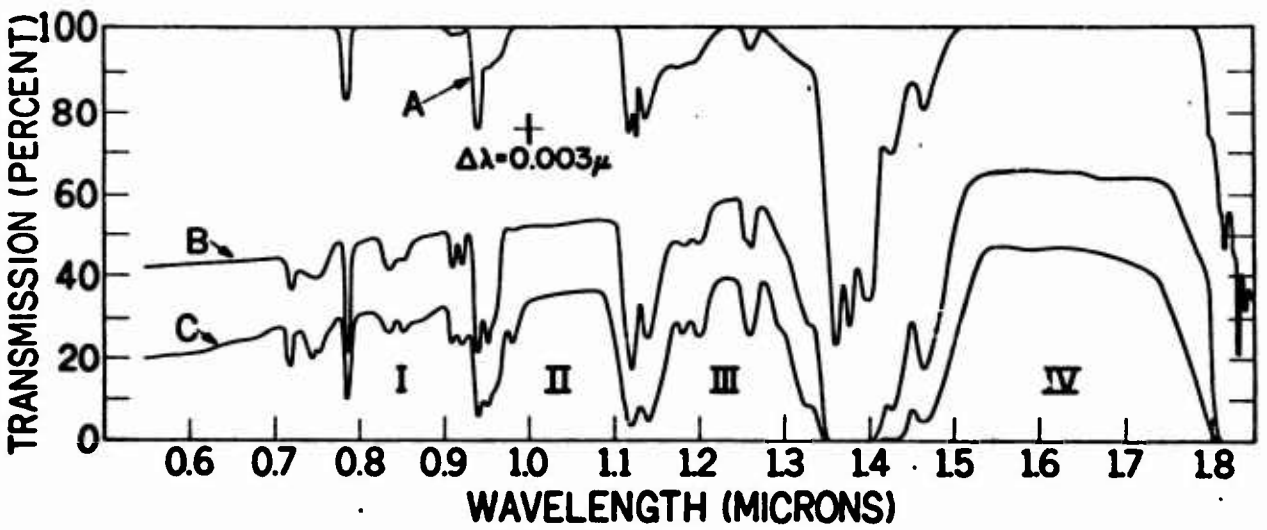

Figure 13. Atmospheric transmission spectra obtained by Taylor and Yates (from reference [51]).

5. SUMMARY AND CONCLUDING REMARKS

The scattering mechanism is of considerable importance in the propagation of 1.06 μm wavelength radiation because this wavelength lies in the 0.92 to 1.10 μm "atmospheric window" of weak molecular absorption. The usual assumption made under these circumstances is that the total extinction coefficient measured in this region of weak molecular absorption is the total scattering coefficient (Rayleigh plus Mie). The contributions by the continuum absorption, aerosol absorption, and selective line absorption are thus assumed negligible. This atmospheric window nonetheless is filled with numerous weak lines [O_2, H_2O, $[O_2]_2$, $[O_2\text{-}N_2]$] whose central frequencies readily absorb laser energy, the aerosol may absorb significantly and the magnitude of the continuum is still undecided. For these reasons the assumption that the total extinction coefficient measured in this window region is the total scattering coefficient is unreasonable for the case of atmospheric attenuation of 1.06 μm laser radiation. To resolve this problem (i.e., account for the various attenuation components in the window regions) the characteristics of the aerosol must be specified, the lines in the atmospheric spectra must be specified to no less than 0.1 cm^{-1} accuracy and the strength of the continuum must be established. For lower accuracy of line positions, errors in the determination of the absorption coefficient may reach tens and hundreds of percent and even higher [31]. For low visibilities (< 10 km), however, the aerosol scattering mechanism will dominate the attenuation of 1.06 μm electromagnetic radiation and, hence, molecular scattering and absorption losses will be of minor significance.

It should be noted that selective window transmission calculations by Berlinguette and Tate [76] were not subjected to the calibration error. Their data showed that for amounts of precipitable water less than 7.4 mm in the path, the transmission in the 0.92 μm to 1.10 μm window is greater than 90%. Hence, the total extinction coefficient in the band 0.92 to 1.10 μm is

$$\gamma_{total} \lesssim 10^{-1}\ km^{-1}.$$

This value seems unreasonably small for total attenuation but appears feasible for the attenuation at the selective wavelength of 1.06 μm.

Also note that Taylor and Yates state the visual range (see Figure 13) in effect at the time of their measurements. A rough, but useful relationship that can be used to estimate the total scattering extinction coefficient, $\beta = \sigma_m + \gamma_a$, for their various sets of measurements is [78]

$$\beta \approx (3.9/V)(0.53/\lambda)^{0.62V^{1/3}} \qquad (34)$$

where V is the visual range expressed in km and λ is the monochromatic beam wavelength in micrometers. The value of $\beta_{1.06}$ for the 5.5 km path length is

$$\beta_{1.06} \sim 4 \times 10^{-2} \text{ km}^{-1}$$

and for the 16.25 km path length is

$$\beta_{1.06} \sim 2 \times 10^{-2} \text{ km}^{-1}.$$

Hence, one might conclude that the scattering mechanism was not as active during the measurements of Taylor and Yates as it was for the measurements of Curcio, Knestrick, Cosden, and Drummeter [59].

If one removes the total scattering component from Taylor and Yate's value for γ_{total} for the 16.25 km path, the following value of γ' results where

$$\gamma'_{1.06} = \gamma_{total} - \beta = 4.3 \times 10^{-2} \text{ km}^{-1}.$$

If the total continuum absorption coefficient is of the order of

$$k_T^c \quad 1.5 \times 10^{-2} \text{ km}^{-1}$$

as discussed previously, then

$$\gamma''_{1.06} = \gamma_{total} - \beta - k^c = 2.8 \times 10^{-2} \text{ km}^{-1}.$$

Hence, it follows that the selective molecular absorption coefficient from Taylor and Yates data for the wavelength 1.06 μm falls in the range

$$2.8 \times 10^{-2} \text{ km}^{-1} < k_m < 6.3 \times 10^{-2} \text{ km}^{-1}$$

when all attenuating mechanisms are taken into account.

In section 2 of this report, the factors that contribute to the atmospheric attenuation of laser energy were identified. These factors are listed in the table below along with numerical values as given in section 3. There is little doubt that for all practical purposes the aerosol is the main attenuating mechanism of 1.06 μm wavelength radiation.

TABLE III MAGNITUDES OF ATMOSPHERIC EFFECTS AT 1.06 μm

Attenuating Mechanism	Attenuation Coefficient Upper Bound (km^{-1})	Attenuation Loss Upper Bound (dB/km)	Reference	Page No. on this Report
Molecular Scattering, σ_m	0.0008	0.003	[19]	12
Selective Molecular Absorption, k_m	0.065	0.282	[49,51]	15
Total Continuum Absorption, k_T^c	0.015	0.065	[55]	25
Aerosol Extinction, γ_a	0.113	0.490	[57]	26
Total Extinction, $\gamma = \sigma_m + k_T^c + k_m + \gamma_a$	0.2	0.87	(clear day, sea level paths)	
Light Rain (1 mm/hr)	0.2	0.87	[71]	32
Heavy Rain (10 mm/hr)	1.2	5.2	[71]	32
Cloudburst (100 mm/hr)	6.3	27.5	[71]	33
Haze	2.3	10	[63]	27
Fog	58	252	[63]	30
Cloud	132	573	[70]	31

The results of this report indicate that the total extinction coefficient at $\lambda = 1.06$ μm for horizontal paths at sea level under good visibility (>10 km) should lie in the range

$$2 \times 10^{-2}\ km^{-1} < \gamma_{total} < 2 \times 10^{-1}\ km^{-1}.$$

The attenuation due to rain over short paths (<5 km) and at low rain rates (<10 mm/hr) is not severe, however, cloud, fog and haze will have a considerable effect on the transmission. The problem regarding the transmission of 1.06 μm vs 1.54 μm is still unresolved. The most definitive statement that can be made at this time is that transmission at these two wavelengths is higher than at most of the other laser wavelengths available.

This study has defined the following areas as barrier problems which need to be resolved before adequate predictions of laser systems performance can be made:

1. Effects of temperature and pressure on the half-widths and intensities of vibrational and rotational lines are not adequately known.

TABLE III MAGNITUDES OF ATMOSPHERIC EFFECTS AT 1.06 μm

Attenuating Mechanism	Attenuation Coefficient Upper Bound (km^{-1})	Attenuation Loss Upper Bound (dB/km)	Reference	Page No. on this Report
Molecular Scattering, σ_m	0.0008	0.003	[19]	12
Selective Molecular Absorption, k_m	0.065	0.282	[49,51]	15
Total Continuum Absorption, k_T^c	0.015	0.065	[55]	25
Aerosol Extinction, γ_a	0.113	0.490	[57]	26
Total Extinction, $\gamma = \sigma_m + k_T^c + k_m + \gamma_a$	0.2	0.87	(clear day, sea level paths)	
Light Rain (1 mm/hr)	0.2	0.87	[71]	32
Heavy Rain (10 mm/hr)	1.2	5.2	[71]	32
Cloudburst (100 mm/hr)	6.3	27.5	[71]	33
Haze	2.3	10	[63]	27
Fog	58	252	[63]	30
Cloud	132	573	[70]	31

The results of this report indicate that the total extinction coefficient at $\lambda = 1.06$ μm for horizontal paths at sea level under good visibility (>10 km) should lie in the range

$$2 \times 10^{-2}\ km^{-1} < \gamma_{total} < 2 \times 10^{-1}\ km^{-1}.$$

The attenuation due to rain over short paths (<5 km) and at low rain rates (<10 mm/hr) is not severe, however, cloud, fog and haze will have a considerable effect on the transmission. The problem regarding the transmission of 1.06 μm vs 1.54 μm is still unresolved. The most definitive statement that can be made at this time is that transmission at these two wavelengths is higher than at most of the other laser wavelengths available.

This study has defined the following areas as barrier problems which need to be resolved before adequate predictions of laser systems performance can be made:

1. Effects of temperature and pressure on the half-widths and intensities of vibrational and rotational lines are not adequately known.

2. Vibration-rotation interaction in computing line spectra needs to be accounted for consistently.

3. Magnitude of continuum absorption is unestablished and its definition is vague.

4. Contribution of $[O_2\text{-}N_2]$ and $[O_2]_2$ complexes to the over-all attenuation at 1.06 μm is uncertain.

5. Aerosol attenuation measurements versus theoretically calculated aerosol coefficients need to be investigated for validity. Controlled experimental measurements in aerosol absorption work are seriously lacking, and research into the altitude variation of the aerosol extinction is urgently needed. In addition, the theoretical treatment of irregular particles needs further investigation.

LITERATURE CITED

1. Vande Kieft, L. J., 1972, "Ground Target Signature Modeling for Artificial Sources," Report No. BRL-1568, Ballistic Research Laboratories, Aberdeen Proving Ground, Maryland. (AD-891 237L)

2. Pratt, H. L., G. A. Emmons, G. H. Widenhofer, and R. T. Gambill, 1971, "Experimental Guidance Laser Designators Employed for the Terminal Homing Flights Tests," Report No. RE-TM-71-3, Directorate for Research, Development, Engineering and Missile Systems Laboratory, U.S. Army MICOM, Redstone Arsenal, Alabama.

3. Roy, E. L., and G. A. Emmons, 1965, "A Literature Survey on the Atmospheric Effects on the Propagation of 1.06 Microns Laser Radiation," Report No. RE-TR-65-3, Electromagnetics Laboratory, U.S. Army MICOM, Redstone Arsenal, Alabama. (AD 461778)

4. Leonard, W. H., G. A. Emmons, H. L. Pratt, and J. S. Kobler, 1971, "Survey of Tactical Measurements Data (U)," Confidential Report No. RB-TN-71-1, U.S. Army MICOM, Redstone Arsenal, Alabama.

5. Ohio State University, 1970, "Effects of the Atmosphere on the Propagation of Laser Radiation," Final Summary Report EES 324X-1, ElectroScience Laboratory, Columbus, Ohio.

6. Long, R. K., 1971, "Comparison of Sea Level Transmittance at 0.56, 0.694, 0.946, 1.06, 1.317, 1.337, 1.536 and 1.544 Microns," Technical Report 2819-2, Ohio State University, ElectroScience Laboratory, Columbus, Ohio.

7. Mak, A. A., Yu. A. Anan'ev, and B. A. Ermakov, 1968, "Solid State Lasers," Soviet Physics USPEKHI, 10, pp. 419-452.

8. Grayson, D. L., and S. J. Weiss, 1970, "Laser Imaging Techniques," NAFI Report No. TR-1615, Applied Research Dept., Naval Avionics Facility, Indianapolis, Indiana, 216 pages.

9. Sylvania Electronics Systems, Electro-Optics Organization, Mountain View, California 94040.

10. Snitzer, E., 1966, "Glass Lasers," Applied Optics, 5, No. 10, pp. 1487-1499.

11. Young, C. G., 1968, "Report on Glass Laser," Microwaves, 7, pp. 69-78.

12. Snitzer, E., and C. G. Young, 1968, "Glass Lasers," Advances in Lasers, 2, A. Levine, Ed. (New York: Dekker), pp. 191-256.

13. Young, C. G., and E. Snitzer, 1968, "Glass Lasers," IEEE J. Quantum Electronics (Digest of Technical Papers), QE-4, p. 360.

14. Young, C. G., 1969, "Glass Lasers," Proceedings of the IEEE, 57, No. 7, pp. 1267-1289.

15. Snitzer, E., 1966, "Frequency Control of A Nd^{3+} Glass Laser," Applied Optics, 5, pp. 121-125.

16. Snitzer, E., 1964, Quantum Electronics III, P. Grivet and N. Bloembergen, Eds. (Columbia University Press, New York) pp. 999.

17. McClatchey, R. A., R. W. Fenn, J. E. A. Selby, J. S. Garing, and F. E. Volz, 1971, "Optical Properties of the Atmosphere (Revised)," Environmental Res. Paper No. 354, Air Force Cambridge Research Laboratories, AFCRL-71-0279, 98 pp. (AD 726 116)

18. Goody, R. M., 1964, Atmospheric Radiation, Vol. I Theoretical Basis, Oxford University Press, London. (See also Zuev, V. E., 1970, "Propagation of Visible and Infrared Waves in the Atmosphere," Izd-vo Sovetskoye Radio, Moscow, 496 pages.)

19. Elterman, L., 1968, "UV, Visible, and IR Attenuation for Altitudes to 50 km, 1968," AFCRL, Environmental Res. Paper No. 285, AFCRL-68-0153.

20. Gucker, F. T., and S. Basu, 1953, "Right-Angle Molecular Scattering from Gases," Science Report No. 1, Contract AF 19(122)-400, University of Indiana.

21. Edlén, B., 1953, "The Dispersion of Standard Air," J. Opt. Soc. Am., 43, No. 5, pp. 339-344.

22. Falcone, V. J., Jr., and R. Dyer, 1970, "Refraction, Attenuation, and Backscattering of Electromagnetic Waves in the Troposphere: A Revision of Chapter 9, Handbook of Geophysics and Space Environments," Air Force Cambridge Research Laboratories, Report No. AFCRL-70-0007, L. G. Hanscom Field, Bedford, Massachusetts.

23. Benedict, W. S., R. Herman, G. E. Moore, and S. Silverman, 1962, "The Strengths, Widths and Shapes of Lines in the Vibration-rotation Bands of CO," Astrophys. J., 135, p. 277.

24. Burch, D. E., D. A. Gryvnak, R. R. Patty, and C. E. Bartky, 1969, "Absorption of Infrared Radiant Energy By CO_2 and H_2O. IV. Shapes of Collision-Broadened CO_2 Lines," J. Opt. Soc. Am., 59, pp. 267-280.

25. Calfee, R. F., 1968, "Anomalous Dispersion Calculated for Atmospheric Water Vapor," Appl. Opt., 7, No. 8, pp. 1652-1654.

26. Burch, D. E., E. B. Singleton, and D. Williams, 1962, "Absorption Line Broadening in the Infrared," Appl. Opt., 1, No. 3, pp. 359-363.

27. Kondrat'yev, K. Ya., and Yu, M. Timofeev, 1966, "Transmission Functions for the Rotational Band of Water Vapor," J. Atmos. Ocean. Phys., (Izv., USSR), 2, No. 3, pp. 162-172.

28. Plass, G. N., and D. I. Fivel, 1955, "The Influence of Variable Mixing Ratio and Temperature on the Radiation Flux," J. Meteor., 12, No. 3.

29. Zuev, V. E., I. I. Ippolitov, Yu. S. Makushkin, A. A. Orlov, and V. V. Fomin, 1968, "The Fine Structure of the Vibrational-Rotational Spectrum of Water Vapor," Soviet Physics, 13, No. 3, pp. 205-207. Translated from Doklady Akademii Nauk USSR, 179, No. 1, pp. 51-54.

30. Gates, D. M., R. F. Calfee, D. W. Hansen, and W. S. Benedict, 1964, "Line Parameters and Computed Spectra for Water Vapor Bands at 2.7 μm," N. B. S. Monograph No. 71, Washington D. C.

31. Moskalenko, N. I., and S. O. Mirumyants, 1970, "Calculation Methods of Spectral Absorption of Infrared Radiation by Atmospheric Gases," J. Atmos. Ocean. Phys., (Izv. USSR) 6, No. 11, pp. 665-675.

32. Zuev, V. E., I. I. Ippolitov, Yu. S. Makushkin, A. A. Orlov, and V. V. Fomin, 1968, "Quantum Mechanical Analysis of the Fine Structure in the Vibrational-Rotation Spectrum of Water Vapor, I. Procedures for the Calculation of Positions, Intensities, and Half-Widths of Lines, and of their Absorption Coefficients," Opt. Spectr., 25, No. 1, pp. 17-21.

33. Andreyev, S. D., and A. P. Gal'tsev, 1970, "Absorption of Infrared Radiation by Water Vapor in Atmospheric Windows," J. Atmos. Ocean. Phys., (Izv., USSR) 6, No. 10, pp. 630-633.

34. Blifford, I. H., Jr. (Ed.), 1971, "Particulate Models; Their Validity and Application," NCAR-TN/PROC-68, Natl. Center for Atmos. Res., Boulder, Colo., 294 pp.

35. Setzer, D. E., 1969, "Comparison of Measured and Predicted Aerosol Scattering Functions," Appl. Opt., 8, No. 3, pp. 905-11.

36. Zuev, V. E., B. P. Koshelev, S. D. Tvorogov, and S. S. Khmelevtsov, 1965, "Attenuation of Visible and Infrared Radiation by Artificial Water Fogs," J. Atmos. Ocean. Phys., (Izv., USSR) 1, No. 3, pp. 298-302.

37. Peterson, J. T., and J. A. Weinman, 1969, "Optical Properties of Quartz Dust Particles at Infrared Wavelengths," J. Geophys. Res., 74, No. 28, pp. 6947-6952.

38. Fenn, R. W., 1964, "Aerosol-Verteilungen and Atmosphärisches Streulicht," Beitr. Phys. Atmos., 34, No. 2, p. 69.

39. Goetz, A., 1957, "An Instrument for the Quantitative Separation and Size Classification of Air-Borne Particulate Matter Down to 0.2 Micron," Geofis. Pura e Appl., 36, pp. 49-69.

40. Kondrat'yev, K. Ya., I. Ya Badinov, L. S. Iviev, and G. A. Nikol'skiy, 1969, "Aerosol Structure of the Troposphere and Stratosphere," J. Atmos. Ocean. Phys., (Izv., USSR) 5, No. 5, pp. 270-276.

41. Rosenburg, G. V., 1968, "Optical Investigations of Atmospheric Aerosol," Soviet Physics, II, No. 3, pp. 353-380. Translated from Inst. of Atmos. Phys., USSR Academy of Sciences, Usp. Fiz. Nauk, 95, pp. 159-208.

42. Winkler, P., 1969, "Untersuchungen über das Grossenwachstum natürlicher Aerosolteilchen mit der Relativen Feuchte nach einer Wägemethode," Ann. Meteorol., NF, No. 4, pp. 134-137.

43. Hänel, G., 1970, "Die Grösse Atmosphärischer Aerosolteilchen als Funktion der Relativen Luftfenchtigkeit," Beitr. Phys. Atmos., 43, pp. 119-132.

44. Junge, C. E., 1963, Air Chemistry and Radioactivity, Academic Press, New York.

45. Foitzik, L., 1965, "The Spectral Extinction of the Atmospheric Aerosol by Mie Particles with Different Gaussian Distributions," Gerlands Beitr. Geophys., 73, Heft 3, pp. 199-206.

46. Van de Hulst, H. C., 1957, Light Scattering by Small Particles, (John Wiley Sons, Inc., New York).

47. Filippov, V. L., and S. O. Mirumyants, 1970, "The Variation of the Spectral Coefficients of Radiation Attenuation by Hazes in the Spectral Region of 0.59-13 μm," J. Atmos. Ocean. Phys., (Izv., USSR) 6, No. 6, pp. 372-374.

48. Rosenberg, G. V., 1967, "The Properties of an Atmospheric Aerosol from Optical Data," J. Atmos. Ocean. Phys., (Izv., USSR) 3, No. 9, pp. 545-552.

49. Mohler, O. C., A. K. Pierce, R. R. McMath, and L. Goldberg, 1950, "Photometric Atlas of the Near Infrared Solar Spectrum λ 8465 to λ 25242," University of Michigan Press, Ann Arbor, Michigan.

50. Migeotte, M., 1961, "Annex to Technical Status Report Number 18," Contract AF 61(512)-962.

51. Taylor, J. H., and H. W. Yates, 1957, "Atmospheric Transmission in the Infrared," J. Opt. Soc. Amer., (Also NRL Report 4759, 2 July 1956).

52. Zuev, V. E., V. V. Polasov, Yu. A. Pkhalagov, A. V. Sosnin, and S. S. Khmelevtosov, 1968, "The Transparency of the Atmospheric Surface Layer to the Radiation of Various Lasers," J. Atmos. Ocean. Phys., (Izv., USSR) 4, No. 1, pp. 32-35.

53. Dianov-Klokov, V. I., and O. A. Matveyeva, 1968, "Absorption Spectrum of Atmospheric Oxygen in the 1.3 - 0.23 μm Region and the Role of Short-Lived $[O_2]_2$, $[O_2\text{-}N_2]$ Complexes," J. Atmos. Ocean. Phys., (Izv., USSR) 4, No. 4, pp. 235-240.

54. Kondrat'yev, K. Ya., I. Ya. Badinov, S. V. Ashcheulov, and S. D. Andreev, 1965, "Some Results of Surface Measurements of the Infrared Absorption and Thermal Radiation Spectra of the Atmosphere," J. Atmos. Ocean. Phys., (Izv., USSR) 1, No. 4, pp. 215-222.

55. Kozyrev, B. P., and V. A. Bazhenov, 1970, "The Absorption of Infrared Radiation by Water Vapor in the Water-Vapor Windows," J. Atmos. Ocean. Phys., (Izv., USSR) 6, No. 6, pp. 375-376.

56. Elder, T., and J. Strong, 1953. "The Infrared Transmission of Atmospheric Windows," J. Franklin Inst., 255, No. 3, pp. 189-208.

57. Streete, J. L., 1968, "Infrared Measurements of Atmospheric Transmission at Sea Level," Appl. Opt., 7, No. 8, pp. 1545-1549.

58. McCormick, M. P., J. D. Lawrence, Jr., and F. R. Crownfield, Jr., 1968, "Mie Total and Differential Backscattering Cross Sections at Laser Wavelengths for Junge Aerosol Models," Appl. Opt., 7, No. 12, pp. 2424-2425.

59. Curcio, J. A., G. L. Knestrick, T. H. Cosden, and L. F. Drummeter, 1961, "The Transmission of Light Signals Beyond the Horizon," US Naval Research Laboratory NRL Report 5676, Washington, D. C. (AD 265925)

60. Knestrick, G. L., T. H. Cosden, and J. A. Curcio, 1962, "Atmospheric Scattering Coefficients in the Visible and Infrared Regions," J. Opt. Soc. Am., 52, No. 9, pp. 1010-1016.

61. Gebbie, H. A., W. R. Harding, C. Helsum, A. W. Pryce, and V. Roberts, 1951, "Atmospheric Transmission in the 1 to 14 μm Region," Proc. Roy. Soc., A, 206, pp. 87-107.

62. Sinclair, D., 1952, Proceedings of the US Technical Conference on Air Pollution, (McGraw-Hill Book Company, Inc.) New York, Chapter 18.

63. Arnulf, A., J. Bricard, E. Curie, and C. Veret, 1957, "Transmission by Haze and Fog in the Spectral Region 0.35 to 10 Microns," J. Opt. Soc. Am., 47, No. 6, pp. 491-498.

64. Robinson, G. D., 1963, "Absorption of Solar Radiation by Atmospheric Aerosol, As Revealed by Measurements at the Ground," Arch. Meteorol. Geophys. Bioklimatol., 12B, pp. 19-40.

65. Kondrat'yev, K. Ya., 1961, Report at the Radiation Symposium, Vienna, (Russian publication).

66. Kurnick, S. W., R. N. Zitter, and D. B. Williams, 1960, "Attenuation of Infrared Radiation by Fogs," J. Opt. Soc. Am., 50, No. 6, pp. 578-583.

67. Barteneva, O. D., and E. A. Polyakova, 1965, "A Study of Attenuation and Scattering of Light in a Natural Fog Due to its Microphysical Properties," J. Atmos. Ocean. Phys., (Izv., USSR) 1, No. 2, pp. 114-121.

68. Johnston, D. R., and D. E. Burch, 1967, "Attenuation by Artificial Fogs in the Visible, Near Infrared, and Far Infrared," Appl. Opt., 6, No. 9, pp. 1497-1501.

69. Gates, D. M., and C. C. Shaw, 1960, "Infrared Transmission of Clouds," J. Opt. Soc. Am., 50, No. 9, pp. 876-882.

70. Carrier, L. W., G. A. Cato, and K. J. von Essen, 1967, "The Backscattering and Extinction of Visible and Infrared Radiation by Selected Major Cloud Models," Appl. Opt., 6, No. 7, pp. 1209-1216.

71. Polyakova, E. A., 1957, "An Experimental Test of the Formula for the Coefficient of Light Attenuation in Rain," Trans. (Trudy); Main Geophysical Observatory, 68. (See also pp. 126-127 Zuev, V. E., "Atmospheric Transparency in the Visible and the Infrared," Soviet Radio Press, 1966, Translated from Russian by Z. Lerman, available from the US Dept of Commerce, Clearinghouse for Federal Scientific and Technical Information, Springfield, Va. 22151.)

72. Wilson, R. W., and A. A. Penzias, 1966, "Effect of Precipitation on Transmission through the Atmosphere at 10 Microns," Nature, 211, No. 5053, p. 1081.

73. Kabanov, M. V., and Yu, A. Pkhalagov, 1970, "The Spectral Transmission of Precipitation in the Infrared," J. Atmos. Ocean. Phys., (Izv., USSR) 6, No. 2, pp. 119-122.

74. Chu, T. S., and D. C. Hogg, 1968, "Effects of Precipitation on Propagation at 0.63, 3.5 and 10.6 Microns," Bell System Tech. J., 47, pp. 723-759.

75. Koprova, L. I., 1968, "The Statistical Characteristics of the Vertical Structure of the Aerosol Attenuation Coefficient," J. Atmos. Ocean. Phys., (Izv., USSR) 4, No. 8, pp. 513-516.

76. Berlinguette, G. E., and P. A. Tate, 1963, "Some Short-Range Narrow-Beam Atmospheric Transmission Measurements in the Near Infrared," Defense Research Chemical Laboratories, Report No. 420, Defense Research Board of Canada, Ottawa.

77. Bruce, R., J. Mason, K. White, and R. B. Gomez, 1968, "An Estimate of the Atmospheric Propagation Characteristics of 1.54 Micron Laser Energy," ECOM-5185, US Army Electronics Command, Atmospheric Sciences Laboratory, White Sands Missile Range, New Mexico. (AD-670934)

78. Bertolotti, M., L. Muzii, and D. Sette, 1969, "On the Possibility of Measuring Optical Visibility by Using a Ruby Laser," Appl. Opt., 8, No. 1, pp. 117-120.

ATMOSPHERIC SCIENCES RESEARCH PAPERS

1. Miers, B. T., and J. E. Morris, Mesospheric Winds Over Ascension Island in January, July 1970, ECOM-5312, AD 711851.
2. Webb, W. L., Electrical Structure of the D- and E-Region, July 1970, ECOM-5313, AD 714365.
3. Campbell, G. S., F. V. Hansen and R. A. Dise, Turbulence Data Derived from Measurements on the 32-Meter Tower Facility, White Sands Missile Range, New Mexico, July 1970, ECOM-5314, AD 711852.
4. Pries, T. H., Strong Surface Wind Gusts at Holloman AFB (March-May), July 1970, ECOM-5315, AD 711853.
5. D'Arcy, E. M., and B. F. Engebos, Wind Effects on Unguided Rockets Fired Near Maximum Range, July 1970, ECOM-5317, AD 711854.
6. Matonis, K., Evaluation of Tower Antenna Pedestal for Weather Radar Set AN/TPS-41, July 1970, ECOM-3317, AD 711520.
7. Monahan, H. H., and M. Armendariz, Gust Factor Variations with Height and Atmospheric Stability, August 1970, ECOM-5320, AD 711855.
8. Stenmark, E. B., and L. D. Drury, Micrometeorological Field Data from Davis, California; 1966-67 Runs Under Non-Advection Conditions, August 1970, ECOM-6051, AD 726390.
9. Stenmark, E. B., and L. D. Drury, Micrometeorological Field Data from Davis, California; 1966-67 Runs Under Advection Conditions, August 1970, ECOM-6052, AD 724612.
10. Stenmark, E. B., and L. D. Drury, Micrometeorological Field Data from Davis, California; 1967 Cooperative Field Experiment Runs, August 1970, ECOM-6053, AD 724613.
11. Rider, L. J., and M. Armendariz, Nocturnal Maximum Winds in the Planetary Boundary Layer at WSMR, August 1970, ECOM-5321, AD 712325.
12. Hansen, F. V., A Technique for Determining Vertical Gradients of Wind and Temperature for the Surface Boundary Layer, August 1970, ECOM-5324, AD 714366.
13. Hansen, F. V., An Examination of the Exponential Power Law in the Surface Boundary Layer, September 1970, ECOM-5326, AD 715349.
14. Miller, W. B., A. J. Blanco and L. E. Traylor, Impact Deflection Estimators from Single Wind Measurements, September 1970, ECOM-5328, AD 716993.
15. Duncan, L. D., and R. K. Walters, Editing Radiosonde Angular Data, September 1970, ECOM-5330, AD 715351.
16. Duncan, L. D., and W. J. Vechione, Vacuum Tube Launchers and Boosters, September 1970, ECOM-5331, AD 715350.
17. Stenmark, E. B., A Computer Method for Retrieving Information on Articles, Reports and Presentations, September 1970, ECOM-6050, AD 724611.
18. Hudlow, M., Weather Radar Investigation on the BOMEX, September 1970, ECOM-3329, AD 714191.
19. Combs, A., Analysis of Low-Level Winds Over Vietnam, September 1970, ECOM-3346, AD 876935.
20. Rinehart, G. S., Humidity Generating Apparatus and Microscope Chamber for Use with Flowing Gas Atmospheres, October 1970, ECOM-5332, AD 716994.
21. Miers, B. T., R. O. Olsen, and E. P. Avara, Short Time Period Atmospheric Density Variations and a Determination of Density Errors from Selected Rocketsonde Sensors, October 1970, ECOM-5335.
22. Rinehart, G. S., Sulfates and Other Water Solubles Larger than 0.15μ Radius in a Continental Nonurban Atmosphere, October 1970, ECOM-5336, AD 716999.
23. Lindberg, J. D., The Uncertainty Principle: A Limitation on Meteor Trail Radar Wind Measurements, October 1970, ECOM-5337, AD 716996.
24. Randhawa, J. S., Technical Data Package for Rocket-Borne Ozone-Temperature Sensor, October 1970, ECOM-5338, AD 716997.

25. Devine, J. C., The Fort Huachuca Climate Calendar, October 1970, ECOM-6054.
26. Allen, J. T., Meteorological Support to US Army RDT&E Activities, Fiscal Year 1970 Annual Report, November 1970, ECOM-6055.
27. Shinn, J. H., An Introduction to the Hyperbolic Diffusion Equation, November 1970, ECOM-5341, AD 718616.
28. Avara, E. P., and M. Kays., Some Aspects of the Harmonic Analysis of Irregularly Spaced Data, November 1970, ECOM-5344, AD 720198.
29. Fabrici, J., Inv. of Isotopic Emitter for Nuclear Barometer, November 1970, ECOM-3349, AD 876461.
30. Levine, J. R., Summer Mesoscale Wind Study in the Republic of Vietnam, December 1970, ECOM-3375, AD 721585.
31. Petriw, A., Directional Ion Anemometer, December 1970, ECOM-3379, AD 720573.
32. Randhawa, J. S., B. H. Williams, and M. D. Kays, Meteorological Influence of a Solar Eclipse on the Stratosphere, December 1970, ECOM-5345, AD 720199.
33. Nordquist, Walter S., Jr., and N. L. Johnson, One-Dimensional Quasi-Time-Dependent Numerical Model of Cumulus Cloud Activity, December 1970, ECOM-5350, AD 722216.
34. Avara, E. P., The Analysis of Variance of Time Series Data Part I: One-Way Layout, January 1971, ECOM-5352, AD 721594.
35. Avara, E. P., The Analysis of Variance of Time Series Data Part II: Two-Way Layout, January 1971, ECOM-5353.
36. Avara, E. P., and M. Kays., The Effect of Interpolation of Data Upon the Harmonic Coefficients, January 1971, ECOM-5354, AD 721593.
37. Randhawa, J. S., Stratopause Diurnal Ozone Variation, January 1971, ECOM-5355, AD 721309.
38. Low, R. D. H., A Comprehensive Report on Nineteen Condensation Nuclei (Part II), January 1971, ECOM-5358.
39. Armendariz, M., L. J. Rider, G. Campbell, D. Favier and J. Serna, Turbulence Measurements from a T-Array of Sensors, February 1971, ECOM-5362, AD 726390.
40. Maynard, H., A Radix-2 Fourier Transform Program, February 1971, ECOM-5363, AD 726389.
41. Devine, J. C., Snowfalls at Fort Huachuca, Arizona, February 1971, ECOM-6056.
42. Devine, J. C., The Fort Huachuca, Arizona 15 Year Base Climate Calendar (1956-1970), February 1971, ECOM-6057.
43. Levine, J. R., Reduced Ceilings and Visibilities in Korea and Southeast Asia, March 1971, ECOM-3403, AD 722735.
44. Gerber, H., et al., Some Size Distribution Measurements of AgI Nuclei with an Aerosol Spectrometer, March 1971, ECOM-3414, AD 729331.
45. Engebos, B. F., and L. J. Rider, Vertical Wind Effects on the 2.75-inch Rocket, March 1971, ECOM-5365, AD 726321.
46. Rinehart, G. S., Evidence for Sulfate as a Major Condensation Nucleus Constituent in Nonurban Fog, March 1971, ECOM-5366.
47. Kennedy, B. W., E. P. Avara, and B. T. Miers, Data Reduction Program for Rocketsonde Temperatures, March 1971, ECOM-5367.
48. Hatch, W. H., A Study of Cloud Dynamics Utilizing Stereoscopic Photogrammetry, March 1971, ECOM-5368.
49. Williamson, L. E., Project Gun Probe Captive Impact Test Range, March 1971, ECOM-5369.
50. Henley, D. C., and G. B. Hoidale, Attenuation and Dispersion of Acoustic Energy by Atmospheric Dust, March 1971, ECOM-5370, AD 728103.
51. Cionco, R. M., Application of the Ideal Canopy Flow Concept to Natural and Artificial Roughness Elements, April 1971, ECOM-5372, AD 730638.
52. Randhawa, J. S., The Vertical Distribution of Ozone Near the Equator, April 1971, ECOM-5373.
53. Ethridge, G. A., A Method for Evaluating Model Parameters by Numerical Inversion, April 1971, ECOM-5374.

54. Collett, E., Stokes Parameters for Quantum Systems, April 1971, ECOM-3415, AD 729347.
55. Shinn, J. H., Steady-State Two-Dimensional Air Flow in Forests and the Disturbance of Surface Layer Flow by a Forest Wall, May 1971, ECOM-5383, AD 730681.
56. Miller, W. B., On Approximation of Mean and Variance-Covariance Matrices of Transformations of Joint Random Variables, May 1971, ECOM-5384, AD 730302.
57. Duncan, L. D., A Statistical Model for Estimation of Variability Variances from Noisy Data, May 1971, ECOM-5385.
58. Pries, T. H., and G. S. Campbell, Spectral Analyses of High-Frequency Atmospheric Temperature Fluctuations, May 1971, ECOM-5387.
59. Miller, W. B., A. J. Blanco, and L. E. Traylor, A Least-Squares Weighted-Layer Technique for Prediction of Upper Wind Effects on Unguided Rockets, June 1971, ECOM-5388, AD 729792.
60. Rubio, R., J. Smith and D. Maxwell, A Capacitance Electron Density Probe, June 1971, ECOM-5390.
61. Duncan, L. D., Redundant Measurements in Atmospheric Variability Experiments, June 1971, ECOM-5391.
62. Engebos, B. F., Comparisons of Coordinate Systems and Transformations for Trajectory Simulations, July 1971, ECOM-5397.
63. Hudlow, M. D., Weather Radar Investigations on an Artillery Test Conducted in the Panama Canal Zone, July 1971, ECOM-5411.
64. White, K. O., E. H. Holt, S. A. Schleusener, and R. F. Calfee, Erbium Laser Propagation in Simulated Atmospheres II. High Resolution Measurement Method, August 1971, ECOM-5398.
65. Waite, R., Field Comparison Between Sling Psychrometer and Meteorological Measuring Set AN/TMQ-22, August 1971, ECOM-5399.
66. Duncan, L. D., Time Series Editing By Generalized Differences, August 1971, ECOM-5400.
67. Reynolds, R. D., Ozone: A Synopsis of its Measurements and Use as an Aemospheric Tracer, August 1971, ECOM-5401.
68. Avara, E. P., and B. T. Miers, Noise Characteristics of Selected Wind and Temperature Data from 30-65 km, August 1971, ECOM-5402.
69. Avara, E. P., and B. T. Miers, Comparison of Linear Trends in Time Series Data Using Regression Analysis, August 1971, ECOM-5403.
70. Miller, W. B., Contributions of Mathematical Structure to the Error Behavior of Rawinsonde Measurements, August 1971, ECOM-5404.
71. Collett, E., Mueller Stokes Matrix Formulation of Fresnel's Equations, August 1971, ECOM-3480.
72. Armendariz, M., and L. J. Rider, Time and Space Correlation and Coherence in the Surface Boundary Layer, September 1971, ECOM-5407.
73. Avara, E. P., Some Effects of Randomization in Hypothesis Testing with Correlated Data, October 1971, ECOM-5408.
74. Randhawa, J. S., Ozone and Temperature Change in the Winter Stratosphere, November 1971, ECOM-5414.
75. Miller, W. B., On Approximation of Mean and Variance-Covariance Matrices of Transformations of Multivariate Random Variables, November 1971, ECOM-5413.
76. Horn, J. D., G. S. Campbell, A. L. Wallis (Capt., USAF), and R. G. McIntyre, Wind Tunnel Simulation and Prototype Studies of Barrier Flow Phenomena, December 1971, ECOM-5416.
77. Dickson, David H., and James R. Oden, Fog Dissipation Techniques for Emergency Use, January 1972, ECOM-5420.
78. Ballard, H. N., N. J. Beyers, B. T. Miers, M. Izquierdo, and J. Whitacre, Atmospheric Tidal Measurements at 50 km from a Constant-Altitude Balloon, December 1971, ECOM-5417.
79. Miller, Walter B., On Calculation of Dynamic Error Parameters for the Rawinsonde and Related Systems, January 1972, ECOM-5422.

80. Richter, Thomas J., Rawin Radar Targets, February 1972, ECOM-5424.
81. Pena, Ricardo, L. J. Rider, and Manuel Armendariz, Turbulence Characteristics at Heights of 1.5, 4.0, and 16.0 Meters at White Sands Missile Range, New Mexico, January 1972, ECOM-5421.
82. Blanco, Abel J., and L. E. Traylor, Statistical Prediction of Impact Displacement due to the Wind Effect on an Unguided Artillery Rocket During Powered Flight, March 1972. ECOM-5427.
83. Williams, B. H., R. O. Olsen, and M. D. Kays, Stratospheric-Ionospheric Interaction During the Movement of a Planetary Wave in January 1967, March 1972, ECOM-5428.
84. Schleusener, Stuart A., and Kenneth O. White, Applications of Dual Parameter Analyzers in Solid-State Laser Tests, April 1972, ECOM-5432.
85. Pries, Thomas H., Jack Smith, and Marvin Hamiter, Some Observations of Meteorological Effects on Optical Wave Propagation, April 1972, ECOM-5434.
86. Dickson, D. H., Fogwash I An Experiment Using Helicopter Downwash, April 1972, ECOM-5431.
87. Mason, J. B., and J. D. Lindberg, Laser Beam Behavior on a Long High Path, April 1972, ECOM-5430.
88. Smith, Jack, Thomas H. Pries, Kenneth J. Skipka, and Marvin Hamiter, Optical Filter Function for a Folded Laser Path, April 1972, ECOM-5433.
89. Lee, Robert P., Artillery Sound Ranging Computer Simulations, May 1972, ECOM-5441.
90. Lowenthal, Marvin J., The Accuracy of Ballistic Density Departure Tables 1934-1972, April 1972, ECOM-5436.
91. Cantor, Israel, Survey of Studies of Atmospheric Transmission from a 4π Light Source to a 2π Receiver, April 1972, ECOM-5435.
92. Barr, William C., Accuracy Requirements for the Measurement of Meteorological Parameters Which Affect Artillery Fire, April 1972, ECOM-5437.
93. Duchon, C. E., F. V. Brock, M. Armendariz, and J. D. Horn, UVW Anemometer Dynamic Performance Study, May 1972, ECOM-5440.
94. Gomez, R. B., Atmospheric Effects for Ground Target Signature Modeling I. Atmospheric Transmission at 1.06 Micrometers, June 1972, ECOM-5445.